

*COST Workshop on
Interplay of hard and soft QCD probes
for collectivity in heavy-ion collisions
Lund, Sweden
25 February – 1 March 2019*



Influence of the electromagnetic fields on hadronic observables in proton-induced collisions

Lucia Oliva

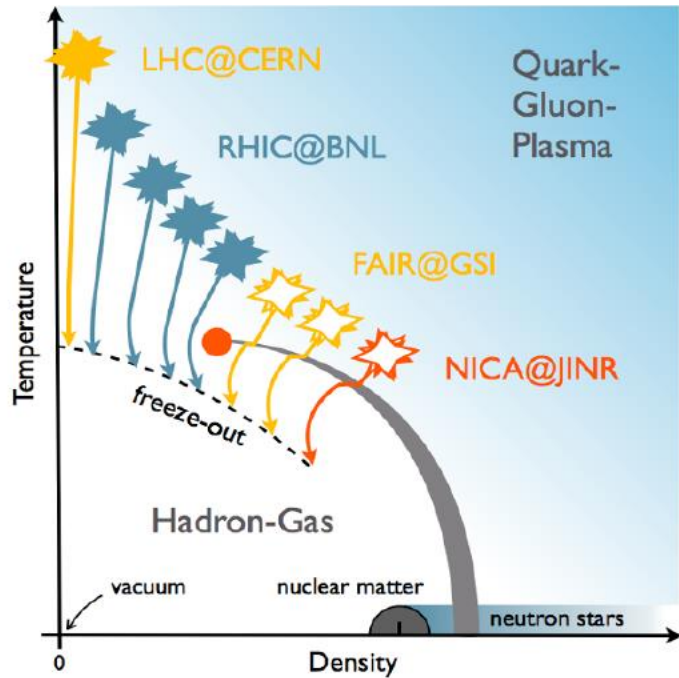
Collaborators: Elena Bratkovskaya, Wolfgang Cassing,
Pierre Moreau, Olga Soloveva, Taesoo Song



Helmholtzzentrum für Schwerionenforschung GmbH



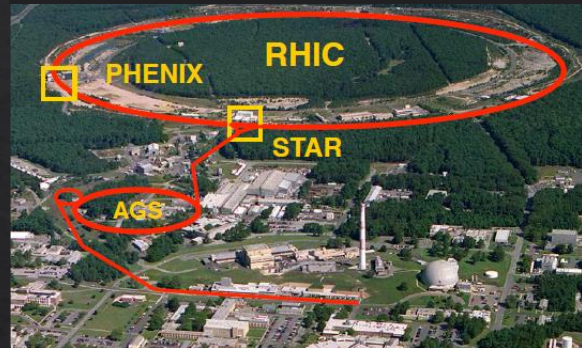
QCD PHASE DIAGRAM



Large Hadron Collider (LHC)



Relativistic Heavy Ion Collider (RHIC)



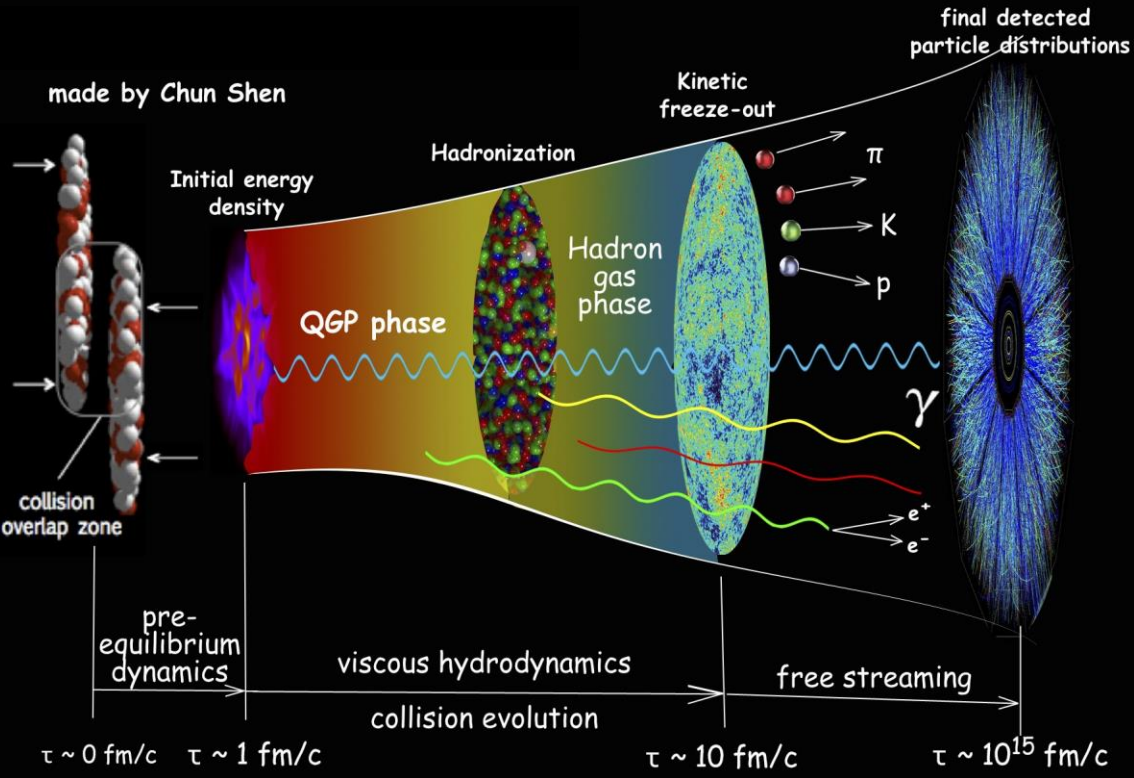
High energy heavy ion collisions

- ✓ allow to experimentally investigate the QCD phase diagram
- ✓ recreate the extreme condition of temperature and density required to form the **QUARK-GLUON PLASMA**

Facility for Antiproton and Ion Research (FAIR)



Nuclotron-based Ion Collider fAcility (NICA)



EXPANDING FIREBALL

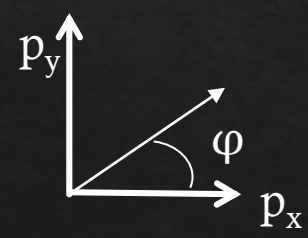
the evolution lasts about
 $t \sim 10\text{-}20 \text{ fm/c} \sim 10^{-23} \text{ s}$

initial temperature is about
 $T \sim 300\text{-}600 \text{ MeV} \sim 10^{12} \text{ K}$

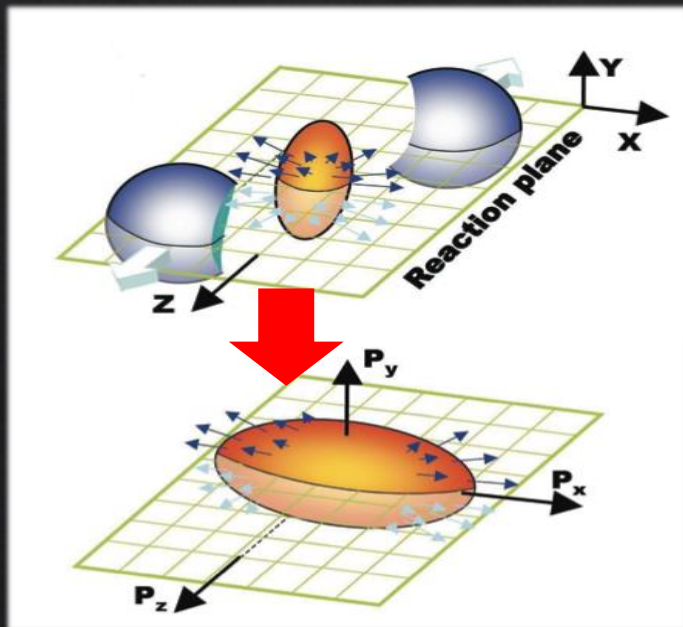
Quark-Gluon Plasma (QGP)

an “almost perfect fluid” with
 very low viscosity and the
 formation of collective flows

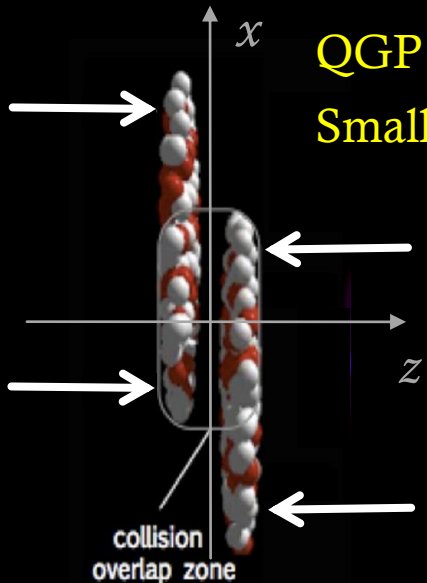
Anisotropic radial flow described
 by the Fourier coefficients of the
 azimuthal particle distributions
 with respect to the reaction plane



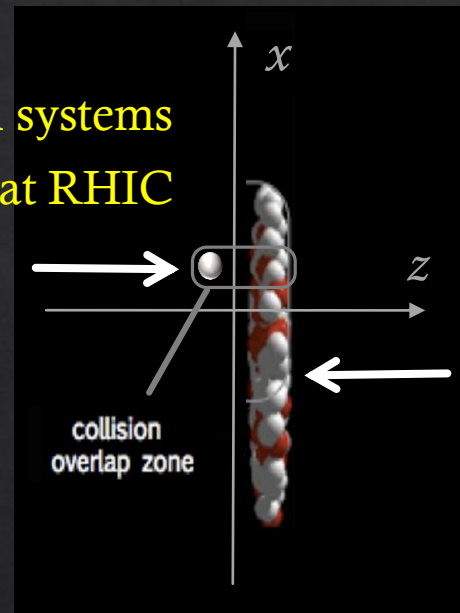
$$\frac{dN}{dp_T d\phi} = \frac{dN}{dp_T} [1 + v_2 \cos(2\phi) + 2v_4 \cos(4\phi) + \dots]$$



QGP initially expected only in high energy collisions of two heavy ions
 Small colliding systems initially regarded as control measurements



Signatures of collective flow found in small systems
 p+Pb collisions at LHC, p/d/³He+Au at RHIC



nature
 physics

LETTERS

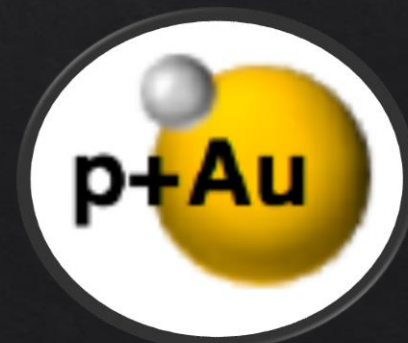
<https://doi.org/10.1038/s41567-018-0360-0>

Creation of quark-gluon plasma droplets with three distinct geometries

PHENIX Collaboration¹

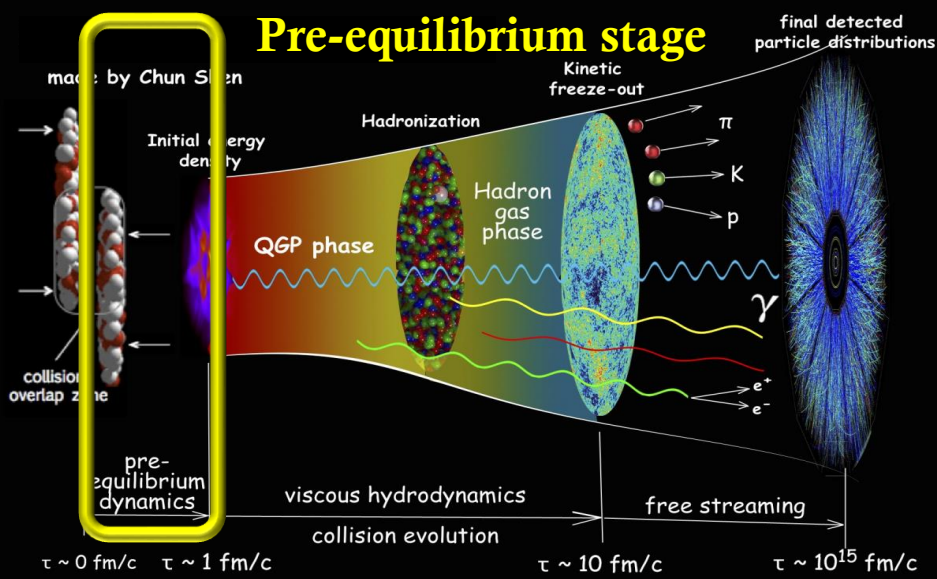
Experimental studies of the collisions of heavy nuclei at relativistic energies have established the properties of the quark-gluon plasma (QGP), a state of hot, dense nuclear matter in which quarks and gluons are not bound into hadrons¹⁻⁴. In this state, matter behaves as a nearly inviscid fluid⁵ that efficiently translates initial spatial anisotropies into correlated momentum anisotropies among the particles produced, creating a common velocity field pattern known as collective flow. In recent years, comparable momentum anisotropies have been measured in small-system proton-proton (p+p) and proton-nucleus (p+A) collisions, despite expectations that the volume and lifetime of the medium produced would be too small to form a QGP. Here we report on the observation of elliptic and triangular flow patterns of charged particles produced in proton-gold (p+Au), deuteron-gold (d+Au) and helium-gold (³He+Au) collisions at a nucleon-nucleon centre-of-mass energy $\sqrt{s_{NN}} = 200$ GeV. The unique combination of three distinct initial geometries and two flow patterns provides unprecedented model discrimination. Hydrodynamical models, which include the formation of a short-lived QGP droplet, provide the best simultaneous description of these measurements.

**COLLECTIVITY
 IN SMALL SYSTEMS
 AS SIGN OF
 QGP DROPLETS?**



proton-induced collisions

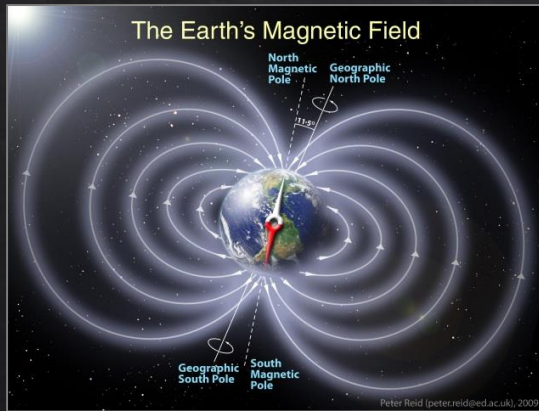
Pre-equilibrium stage



Intense magnetic field

$$eB_y \sim 5-50 m_\pi^2 \sim 10^{18}-10^{19} \text{ G}$$

Kharzeev, McLerran and Warringa, NPA 803 (2008) 227
 Skokov, Illarionov and Toneev, IJMPA 24 (2009) 5925



Earth's magnetic field
 $\sim 1 \text{ G}$



laboratory
 $\sim 10^6 \text{ G}$



magnetar
 $\sim 10^{14}-10^{15} \text{ G}$

PHSD: Parton-Hadron-String Dynamics

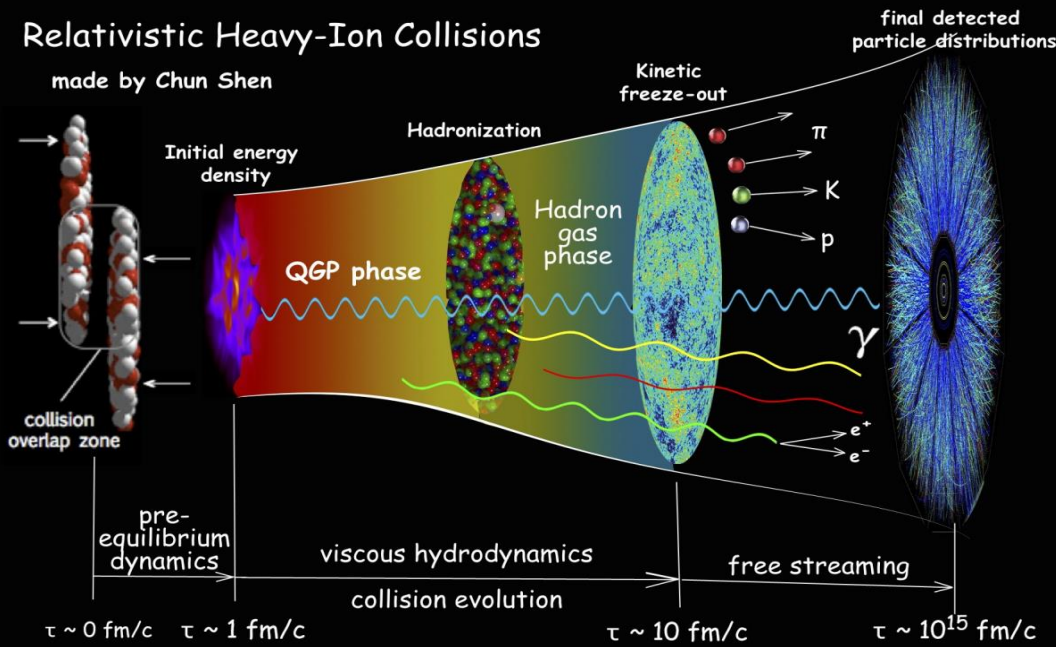
A consistent non-equilibrium transport approach to study heavy ion collisions (HICs) on a microscopic level

Cassing and Bratkovskaya, PRC 78 (2008) 034919; NPA831 (2009) 215
Cassing, EPJ ST 168 (2009) 3; NPA856 (2011) 162



Relativistic Heavy-Ion Collisions

made by Chun Shen



GOAL

study the phase transition from hadronic to partonic matter and the properties of the quark gluon plasma from a microscopic origin

PHSD: Parton-Hadron-String Dynamics

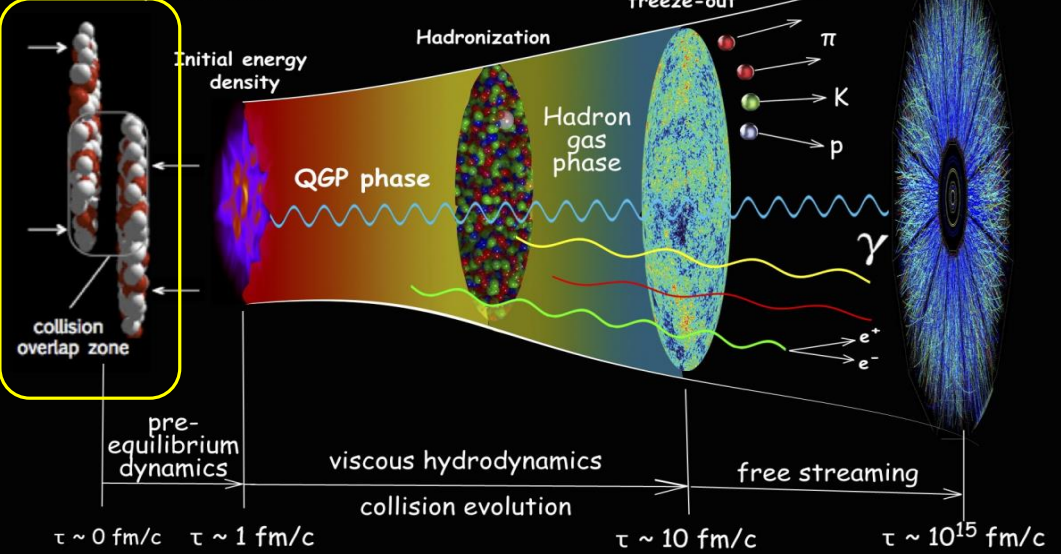
A consistent non-equilibrium transport approach to study heavy ion collisions (HICs) on a microscopic level



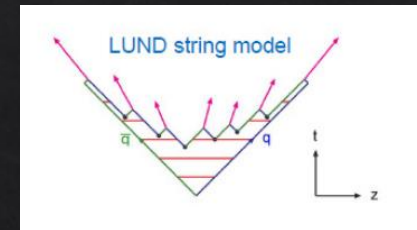
Cassing and Bratkovskaya, PRC 78 (2008) 034919; NPA831 (2009) 215
Cassing, EPJ ST 168 (2009) 3; NPA856 (2011) 162

Relativistic Heavy-Ion Collisions

made by Chun Shen



- string formation in primary nucleon-nucleon collisions
- string decay to pre-hadrons (baryons and mesons)



INITIAL A+A COLLISIONS

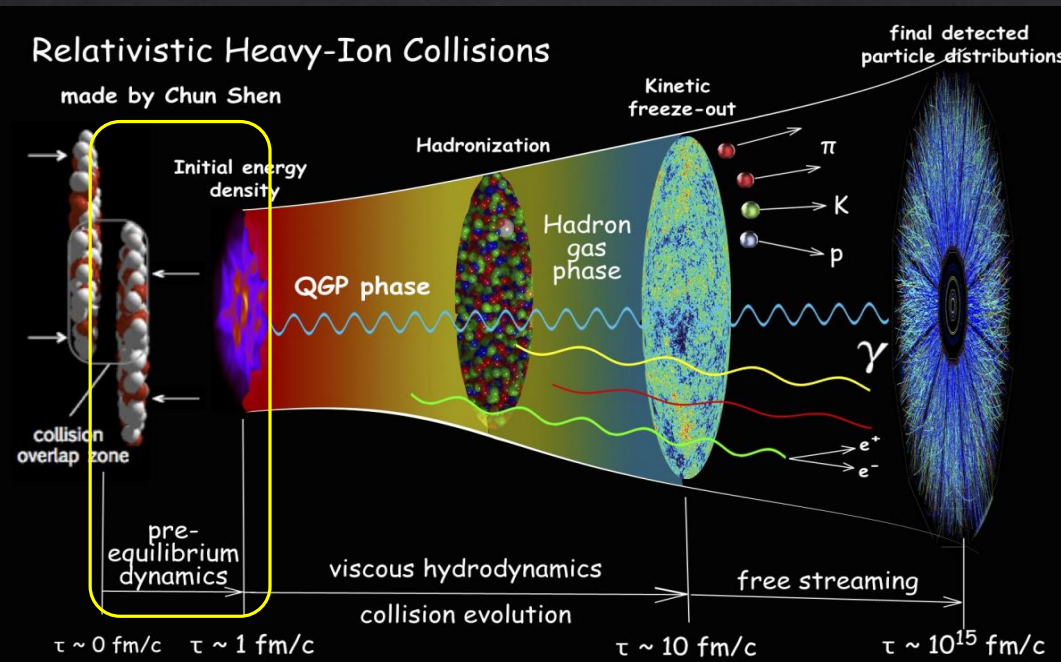
nucleon-nucleon collisions between the two incoming nuclei lead to the formation of strings that decay to pre-hadrons

PHSD: Parton-Hadron-String Dynamics

A consistent non-equilibrium transport approach to study heavy ion collisions (HICs) on a microscopic level



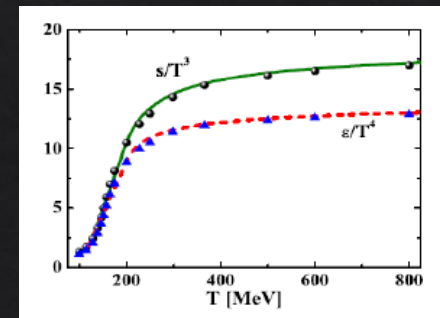
Cassing and Bratkovskaya, PRC 78 (2008) 034919; NPA831 (2009) 215
 Cassing, EPJ ST 168 (2009) 3; NPA856 (2011) 162



- the Dynamical Quasi-Particle Model (DQPM) defines parton spectral functions, i.e. masses $M_{q,g}(\epsilon)$ and widths $\Gamma_{q,g}(\epsilon)$
- mean-field potential U_q at given ϵ related by lQCD EoS to the local temperature

FORMATION OF QUARK-GLUON PLASMA

if the energy density is above the critical value
 pre-hadrons dissolve in massive quarks and gluons

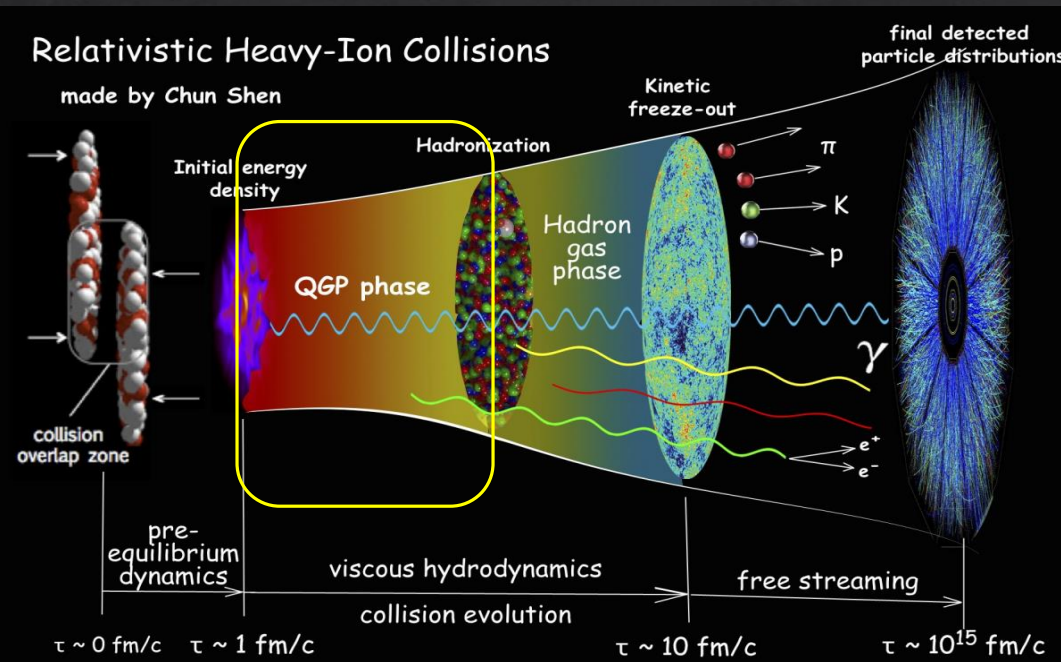


PHSD: Parton-Hadron-String Dynamics

A consistent non-equilibrium transport approach to study heavy ion collisions (HICs) on a microscopic level



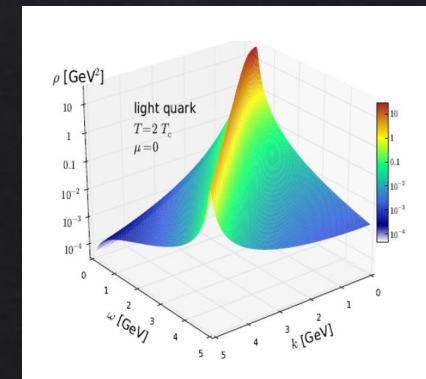
Cassing and Bratkovskaya, PRC 78 (2008) 034919; NPA831 (2009) 215
 Cassing, EPJ ST 168 (2009) 3; NPA856 (2011) 162



- quarks and gluons as ‘dynamical quasiparticles’ with off-shell spectral functions
- self-generated mean-field potential
- Equation of state from lattice QCD
- (quasi-)elastic and inelastic parton-parton interactions

PARTONIC STAGE

evolution based on off-shell transport equations and the Dynamical Quasi-Particle Model (DQPM)

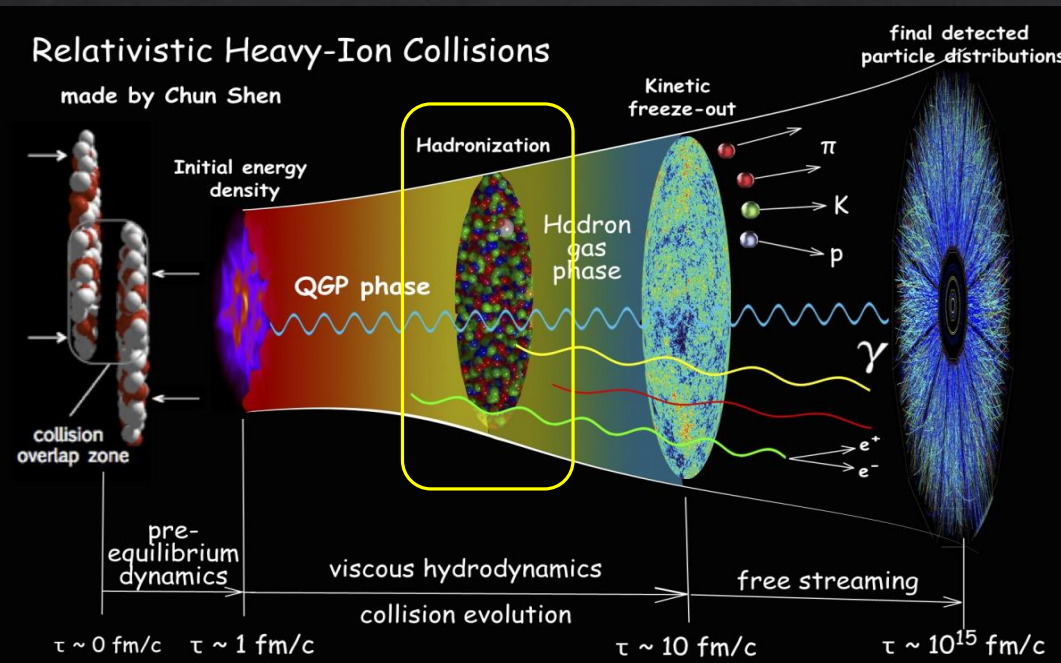


PHSD: Parton-Hadron-String Dynamics

A consistent non-equilibrium transport approach to study heavy ion collisions (HICs) on a microscopic level



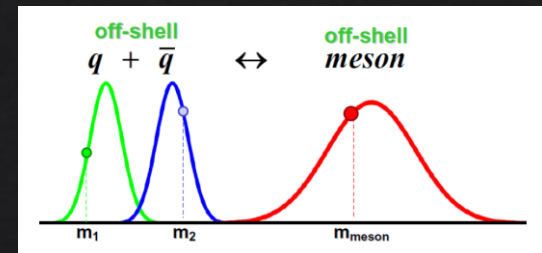
Cassing and Bratkovskaya, PRC 78 (2008) 034919; NPA831 (2009) 215
 Cassing, EPJ ST 168 (2009) 3; NPA856 (2011) 162



- massive off-shell quarks and antiquarks with broad spectral functions hadronize to off-shell mesons and baryons or strings
- local covariant off-shell transition rate for $q + \bar{q}$ fusion which lead to meson formation

HADRONIZATION

massive off-shell quarks with broad spectral functions hadronize to off-shell mesons and baryons

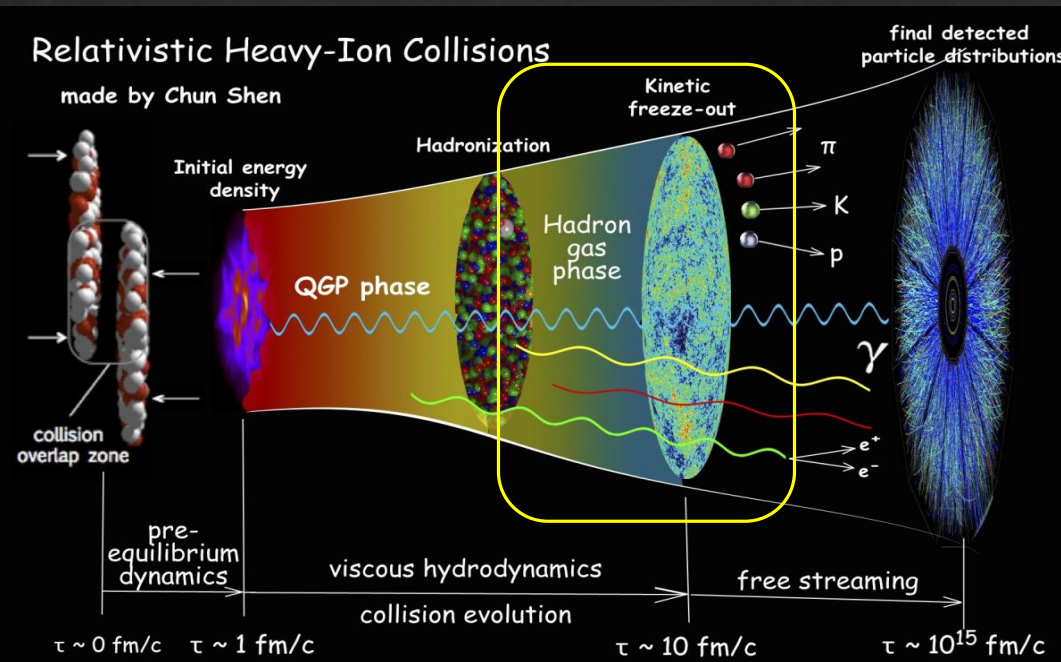


PHSD: Parton-Hadron-String Dynamics

A consistent non-equilibrium transport approach to study heavy ion collisions (HICs) on a microscopic level



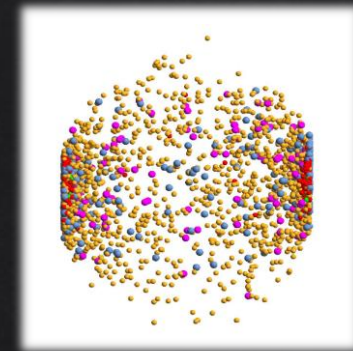
Cassing and Bratkovskaya, PRC 78 (2008) 034919; NPA831 (2009) 215
Cassing, EPJ ST 168 (2009) 3; NPA856 (2011) 162



- off-shell propagation
- elastic and inelastic hadron-hadron interactions

HADRONIC PHASE

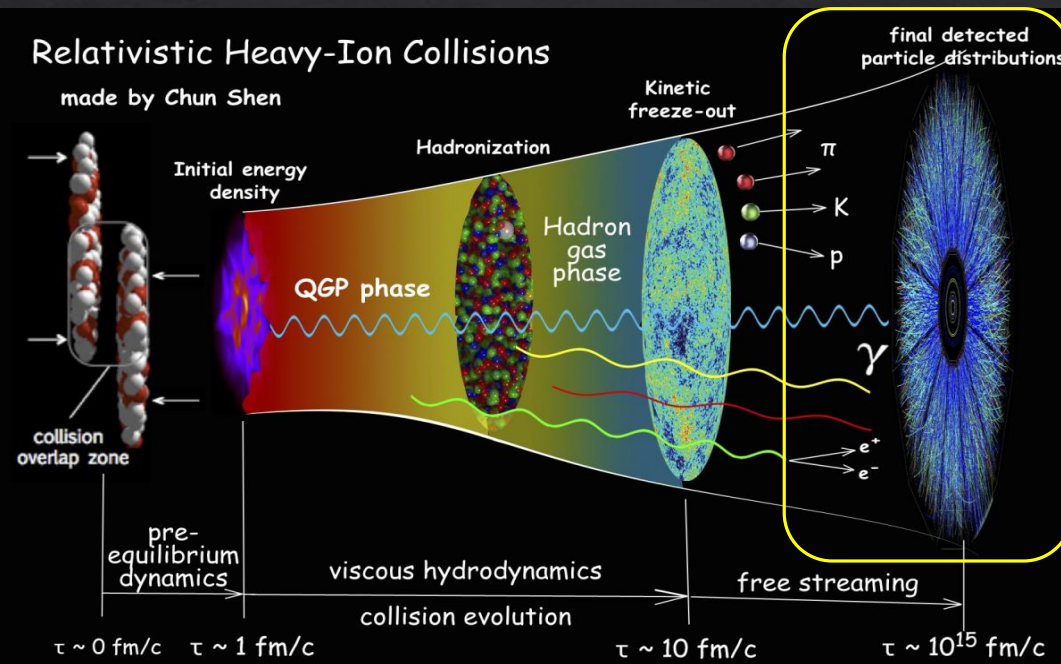
evolution based on off-shell transport equations with hadron-hadron interactions



PHSD: Parton-Hadron-String Dynamics

A consistent non-equilibrium transport approach to study heavy ion collisions (HICs) on a microscopic level

Cassing and Bratkovskaya, PRC 78 (2008) 034919; NPA831 (2009) 215
Cassing, EPJ ST 168 (2009) 3; NPA856 (2011) 162



FINAL OBSERVABLES

good description of bulk observables (rapidity and transverse momentum distributions, flow coefficients, ...) for A+A collisions from SPS to LHC energies

PHSD + electromagnetic fields



PHSD includes the dynamical formation and evolution of the retarded electromagnetic field (EMF) and its influence on the quasi-particle (QP) dynamics

Voronyuk *et al.*, PRC 83 (2011) 054911

Toneev *et al.*, PRC 85 (2012) 034910; PRC 86 (2012) 064907; PRC 95 (2017) 034911

TRANSPORT EQUATION

$$\left\{ \frac{\partial}{\partial t} + \left(\frac{\mathbf{p}}{p_0} + \nabla_{\mathbf{p}} U \right) \nabla_{\mathbf{r}} + (-\nabla_{\mathbf{r}} U + e\mathbf{E} + e\mathbf{v} \times \mathbf{B}) \nabla_{\mathbf{p}} \right\} f = C_{\text{coll}}(f, f_1, \dots, f_N)$$

Lorentz force

MAXWELL EQUATIONS

$$\nabla \cdot \mathbf{B} = 0 \quad \nabla \times \mathbf{E} = -\frac{\partial \mathbf{B}}{\partial t} \quad \nabla \cdot \mathbf{E} = 4\pi\rho \quad \nabla \times \mathbf{B} = \frac{\partial \mathbf{E}}{\partial t} + \frac{4\pi}{c}\mathbf{j}$$

charge distribution

electric current

consistent solution of particle and field evolution equations

Retarded electromagnetic fields

$$\mathbf{B} = \nabla \times \mathbf{A}, \quad \mathbf{E} = -\nabla\Phi - \frac{\partial\mathbf{A}}{\partial t}$$

General solution of the wave equation for the electromagnetic potentials

$$\mathbf{A}(\mathbf{r}, t) = \frac{1}{4\pi} \int \frac{\mathbf{j}(\mathbf{r}', t') \delta(t - t' - |\mathbf{r} - \mathbf{r}'|/c)}{|\mathbf{r} - \mathbf{r}'|} d^3r' dt'$$

$$\Phi(\mathbf{r}, t) = \frac{1}{4\pi} \int \frac{\rho(\mathbf{r}', t') \delta(t - t' - |\mathbf{r} - \mathbf{r}'|/c)}{|\mathbf{r} - \mathbf{r}'|} d^3r' dt'$$

$$\mathbf{r}' \equiv \mathbf{r}(t')$$

$$t' = t - \frac{|\mathbf{r} - \mathbf{r}'|}{c}$$

Liénard-Wiechert potentials for a moving point-like charge

$$\Phi(\mathbf{r}, t) = \frac{e}{4\pi} \left[\frac{1}{R(1 - \mathbf{n} \cdot \boldsymbol{\beta})} \right]_{\text{ret}} \quad \mathbf{A}(\mathbf{r}, t) = \frac{e}{4\pi} \left[\frac{\boldsymbol{\beta}}{R(1 - \mathbf{n} \cdot \boldsymbol{\beta})} \right]_{\text{ret}}$$

ret: evaluated at the times t'

$$\mathbf{R} = \mathbf{r} - \mathbf{r}'$$

$$\mathbf{n} = \frac{\mathbf{R}}{R}$$

$$\boldsymbol{\beta} = \frac{\mathbf{v}}{c}$$

Retarded electromagnetic fields

Retarded electric and magnetic fields for a moving point-like charge

$$\mathbf{E}(\mathbf{r}, t) = \frac{e}{4\pi} \left[\frac{\mathbf{n} - \boldsymbol{\beta}}{(1 - \mathbf{n} \cdot \boldsymbol{\beta})^3 \gamma^2 R^2} + \frac{\mathbf{n} \times ((\mathbf{n} - \boldsymbol{\beta}) \times \dot{\boldsymbol{\beta}})}{(1 - \mathbf{n} \cdot \boldsymbol{\beta})^3 cR} \right]_{\text{ret}} \quad \mathbf{B}(\mathbf{r}, t) = [\mathbf{n} \times \mathbf{E}(\mathbf{r}, t)]_{\text{ret}}$$

elastic Coulomb
scatterings

inelastic bremsstrahlung
processes

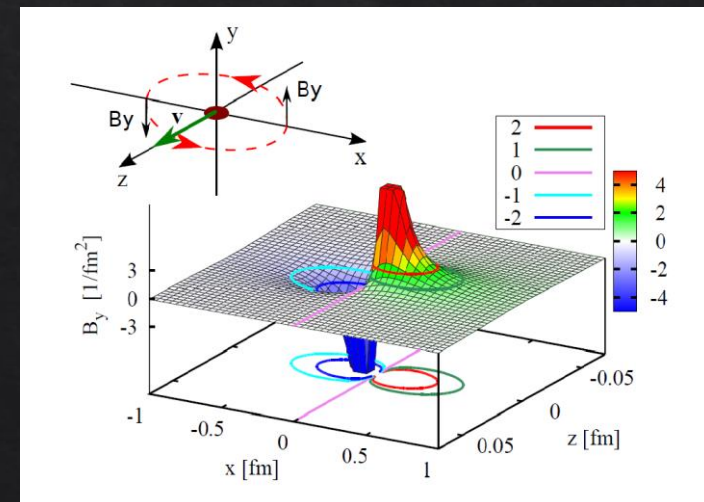
$$\mathbf{R} = \mathbf{r} - \mathbf{r}' \quad \mathbf{n} = \frac{\mathbf{R}}{R} \quad \boldsymbol{\beta} = \frac{\mathbf{v}}{c}$$

magnetic field created by a
single freely moving charge

Neglecting the acceleration

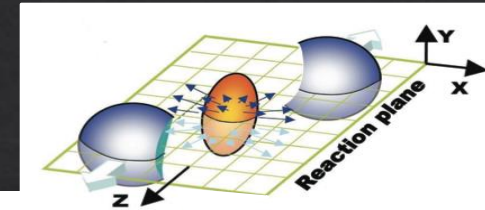
$$e\mathbf{E}(t, \mathbf{r}) = \alpha_{em} \frac{1 - \beta^2}{[(\mathbf{R} \cdot \boldsymbol{\beta})^2 + R^2(1 - \beta^2)]^{3/2}} \mathbf{R}$$

$$e\mathbf{B}(t, \mathbf{r}) = \alpha_{em} \frac{1 - \beta^2}{[(\mathbf{R} \cdot \boldsymbol{\beta})^2 + R^2(1 - \beta^2)]^{3/2}} \boldsymbol{\beta} \times \mathbf{R}$$



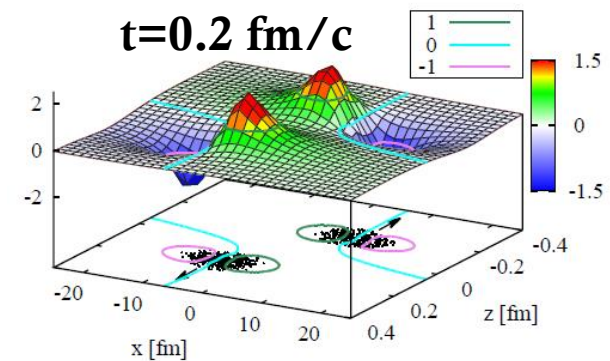
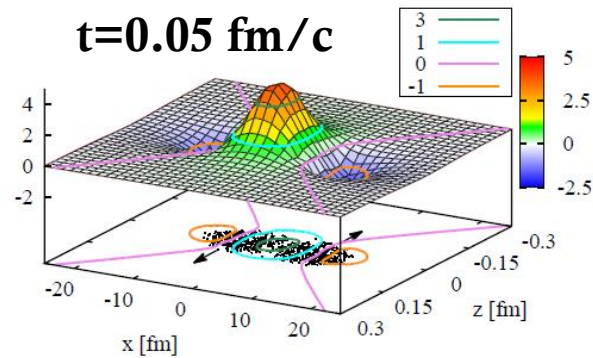
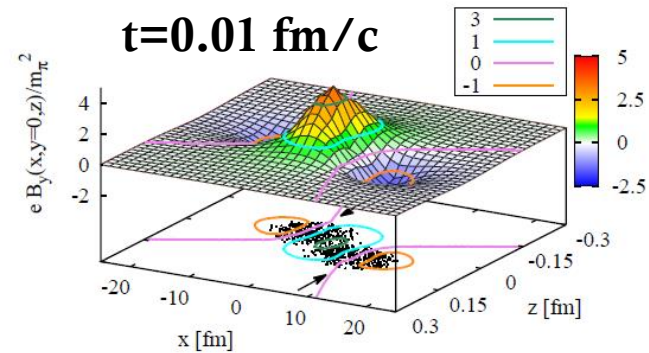
EM fields in nuclear collisions

in a nuclear collision the magnetic field is a superposition of solenoidal fields from different moving charges



Voronyuk *et al.* (PHSD team), PRC 83 (2011) 054911

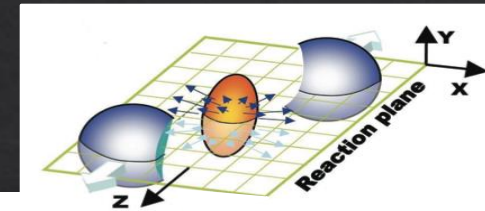
Au+Au @RHIC 200 GeV - $b = 10$ fm



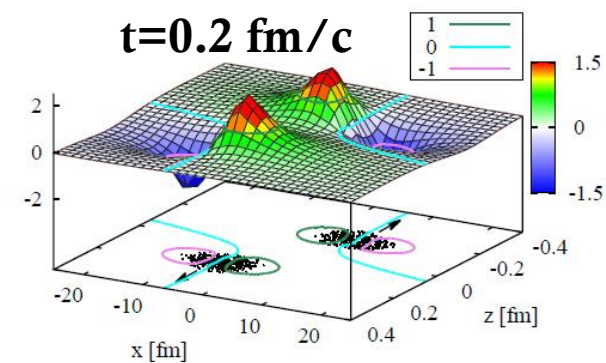
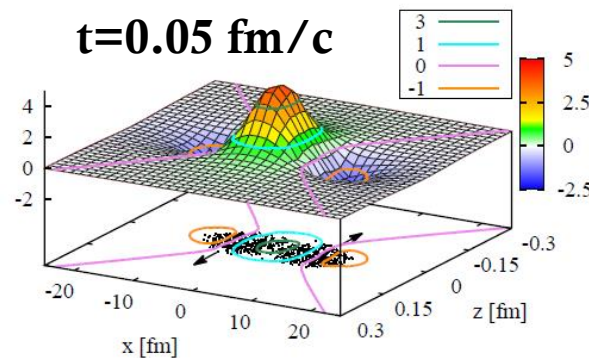
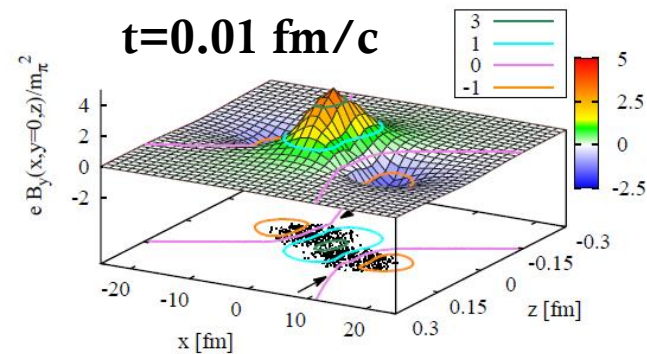
EM fields in nuclear collisions

in a nuclear collision the magnetic field is a superposition of solenoidal fields from different moving charges

Voronyuk *et al.* (PHSD team), PRC 83 (2011) 054911



Au+Au @RHIC 200 GeV – $b = 10$ fm



❖ SYMMETRIC SYSTEMS (Au+Au, Pb+Pb)

transverse momentum increments due to electric and magnetic fields partially compensate each other

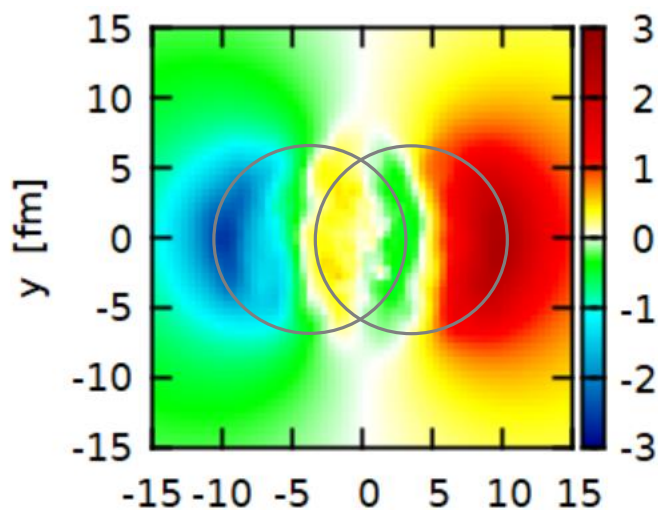
❖ ASYMMETRIC SYSTEMS (e.g. Cu+Au, p+Au)

electric field strongly asymmetric inside the overlap region

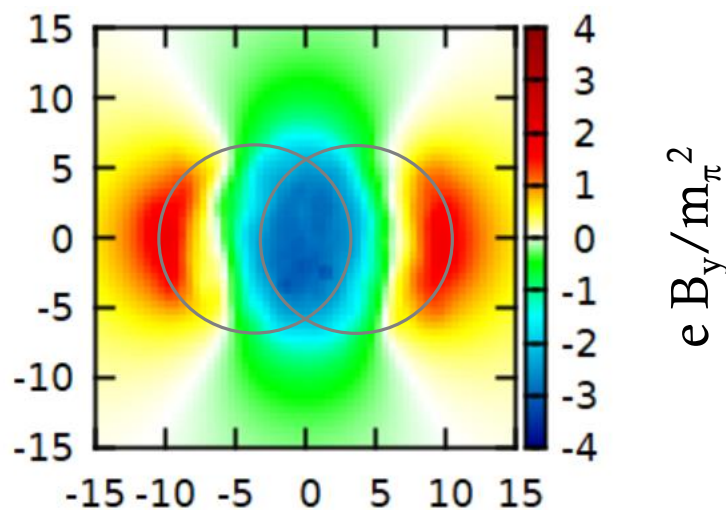
Voronyuk *et al.* (PHSD team), PRC 90, 064903 (2014)

EM fields in proton-induced collisions

*Au+Au
collisions
@RHIC
200GeV
b=7 fm*

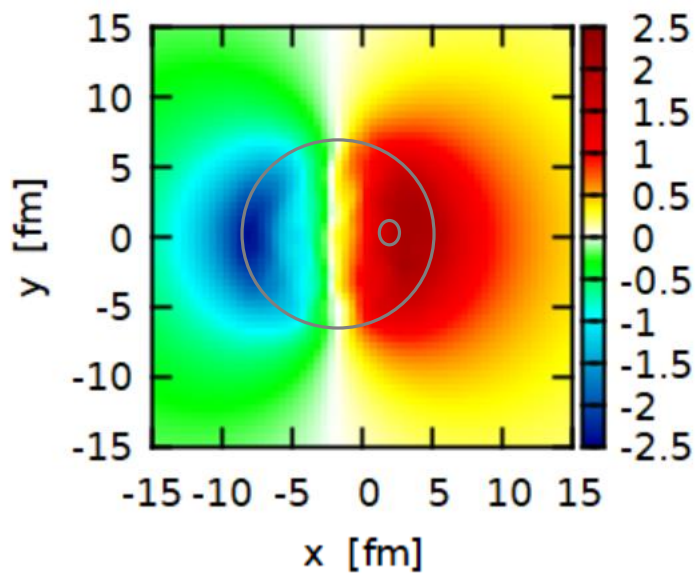


$e E_x / m_\pi^2$

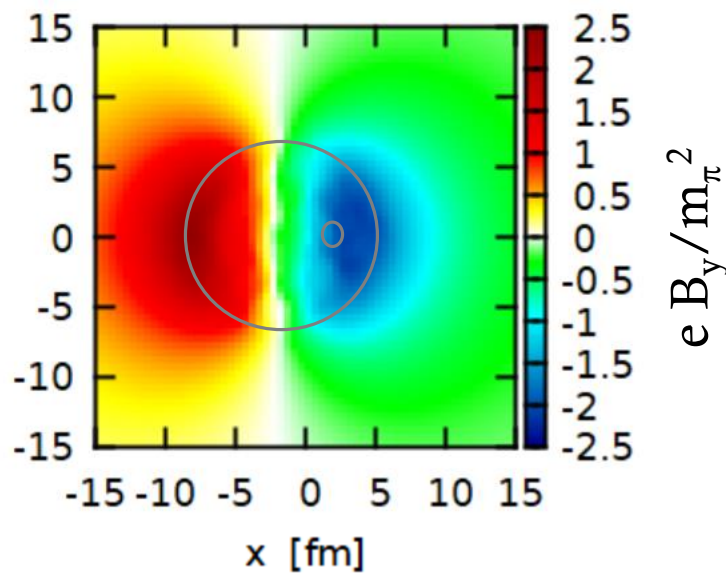


$e B_y / m_\pi^2$

*p+Au
collisions
@RHIC
200GeV
b=4 fm*

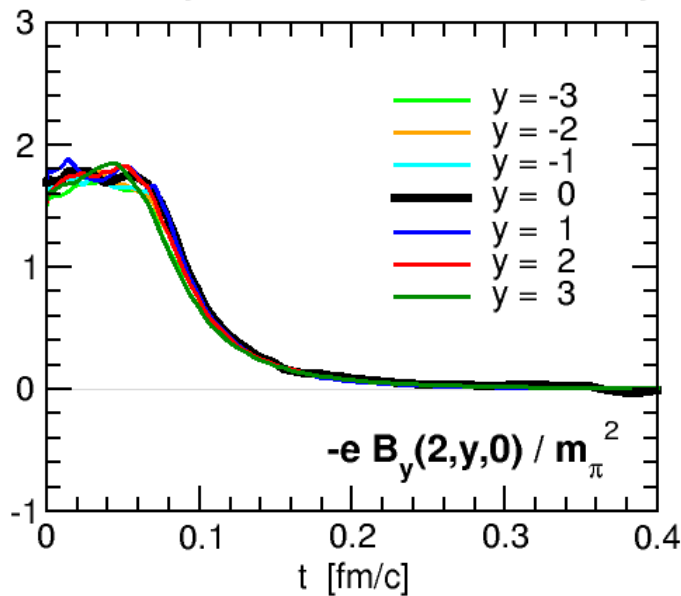
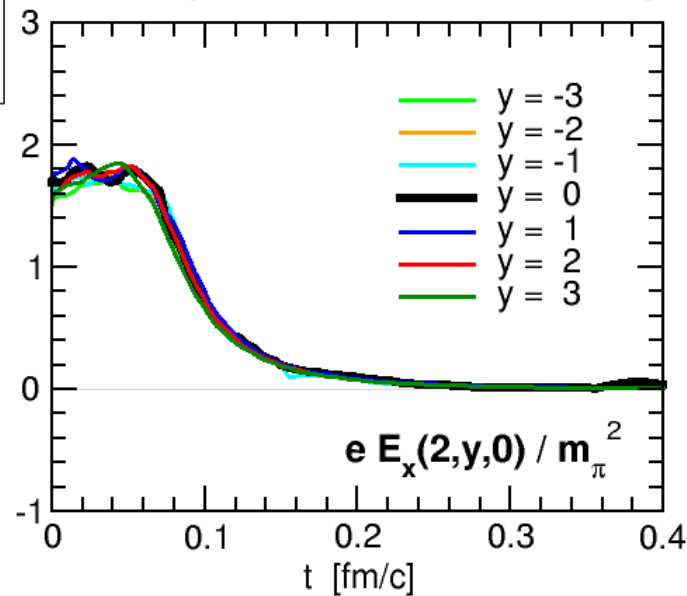
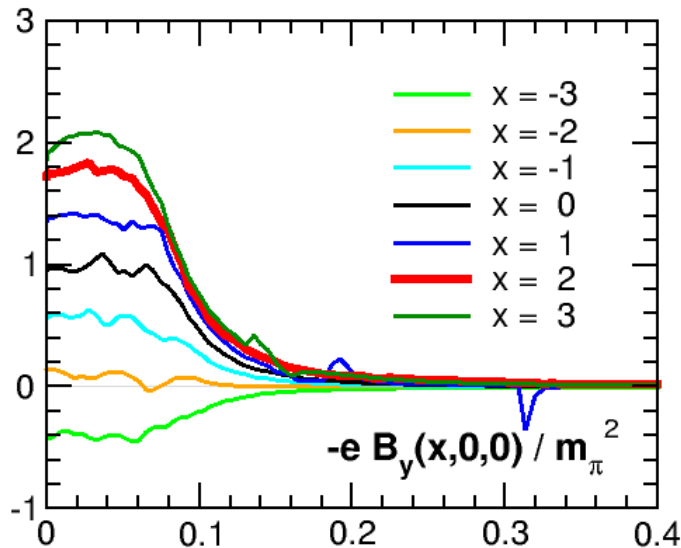
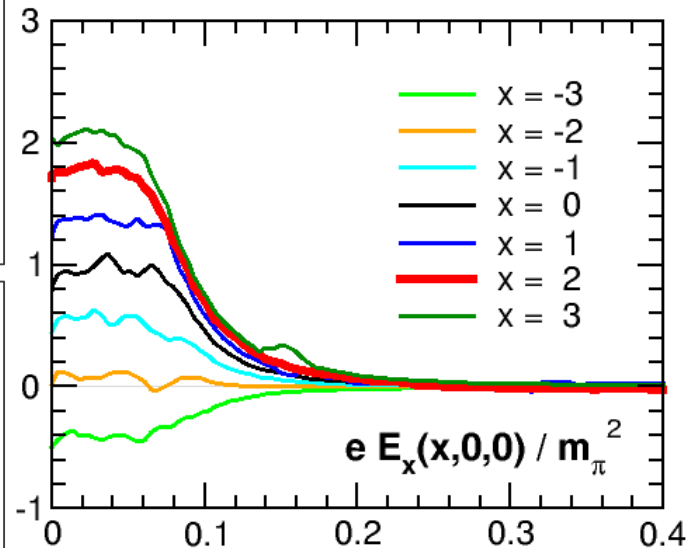
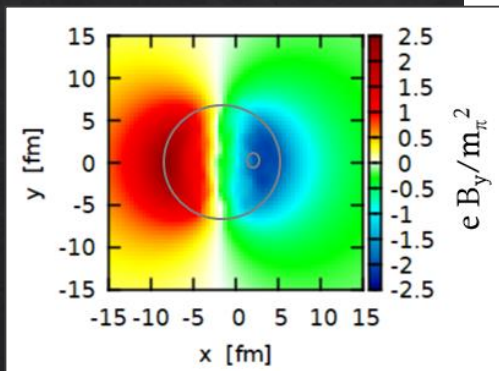
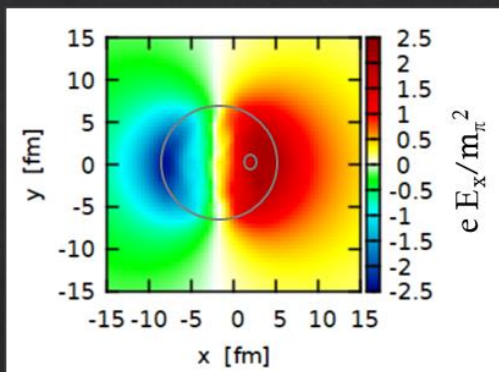


$e E_x / m_\pi^2$



$e B_y / m_\pi^2$

EM fields in proton-induced collisions



p+Au
collisions
@RHIC
200GeV
 $b=4$ fm

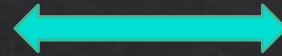
Centrality in heavy ion collisions

Centrality characterizes the amount of overlap or size of the fireball in the collision region

e.g. (MC-)Glauber model

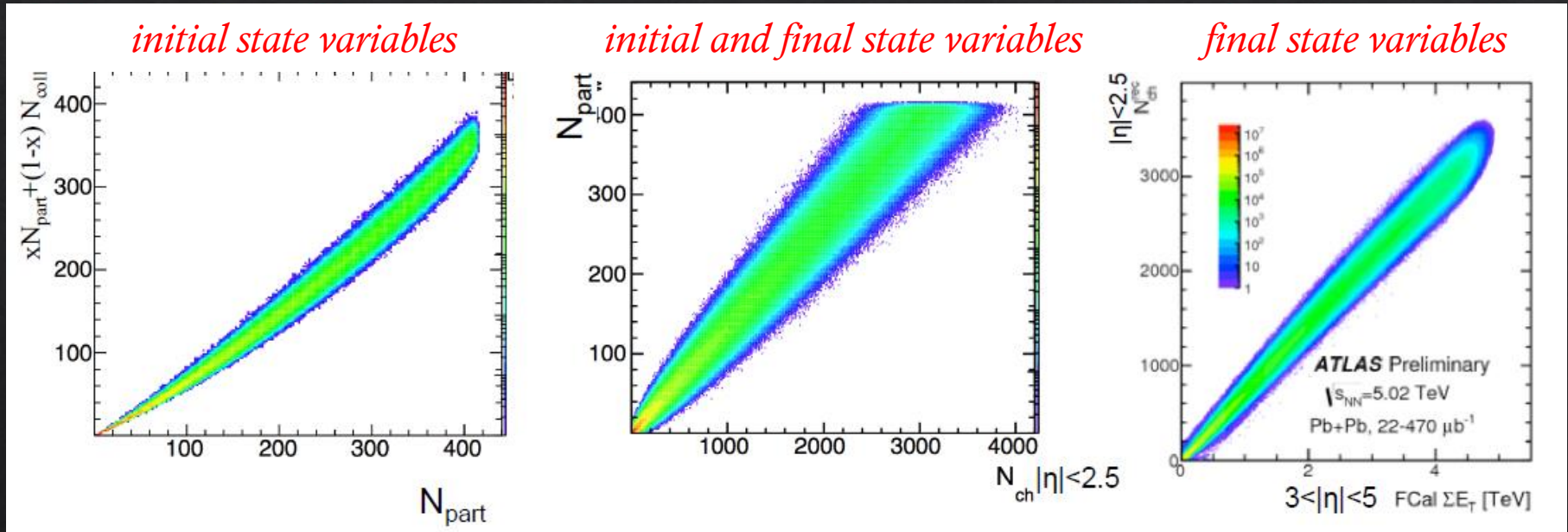
INITIAL STATE QUANTITIES

$b, N_{\text{part}}, \{N_{\text{part}}, N_{\text{coll}}\}, N_{\text{qp}}$



FINAL STATE OBSERVABLES

$N_{\text{ch}}, E_{\text{T}}, N_{\text{neutron}}$

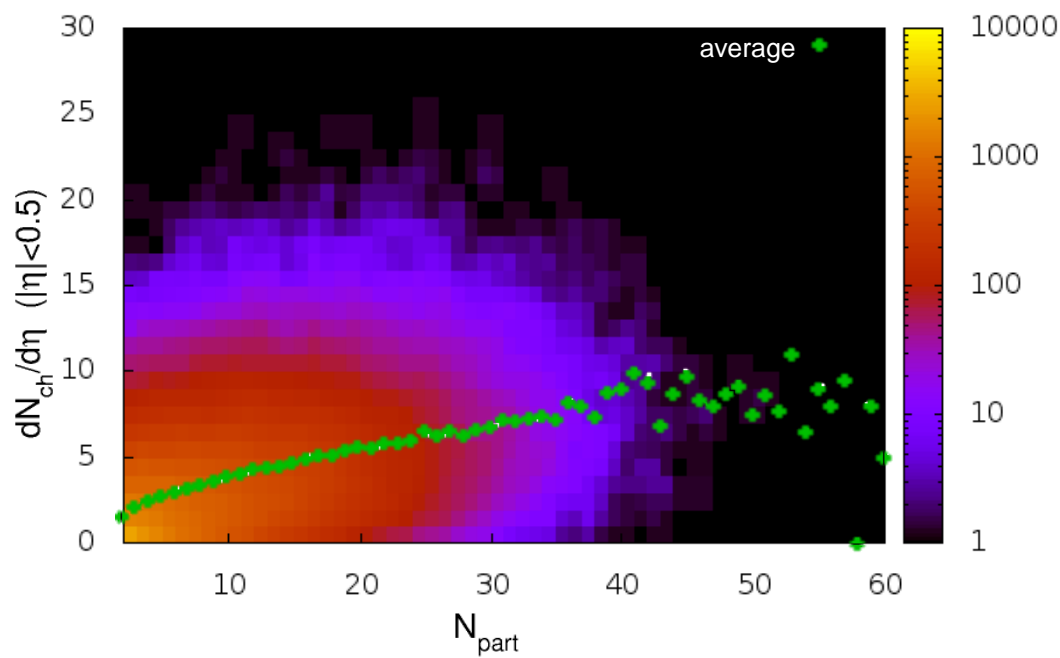


from talk of Jianguong Jia at MIAPP (2018)

CENTRALITY FLUCTUATION

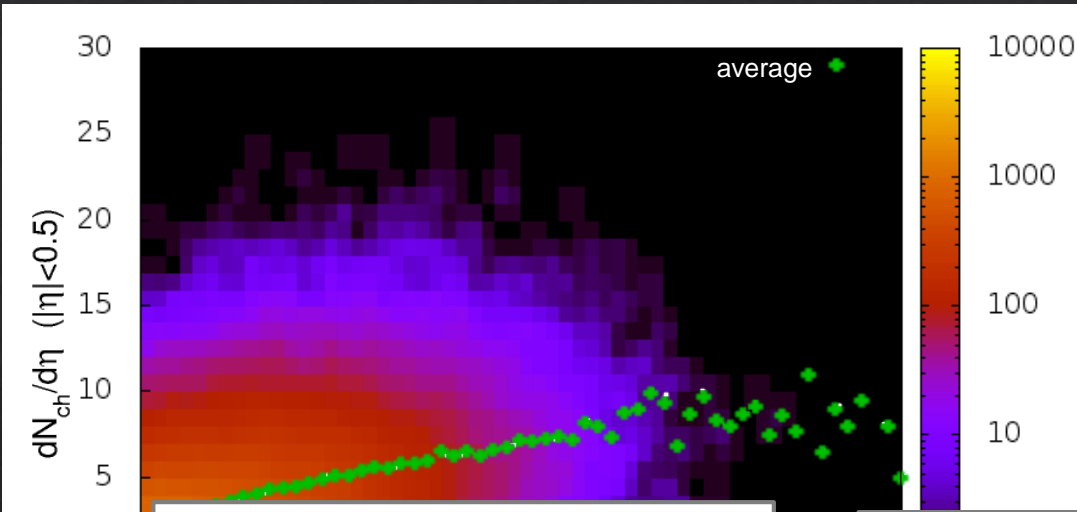
- ❖ main uncertainty for many measurements
- ❖ large in peripheral collisions or small collision systems

p+Au collisions @ RHIC 200 GeV

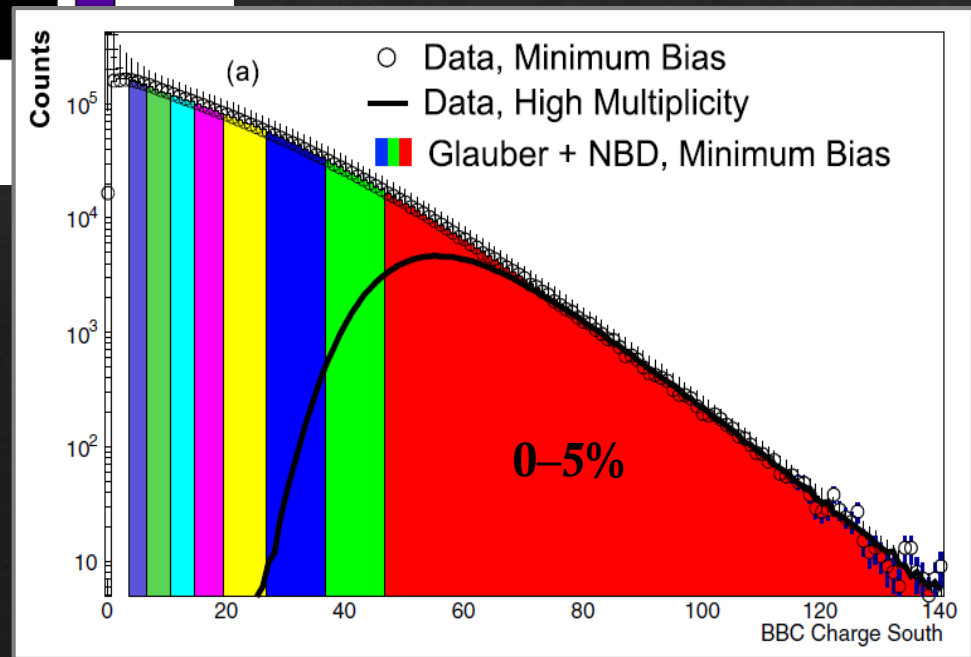
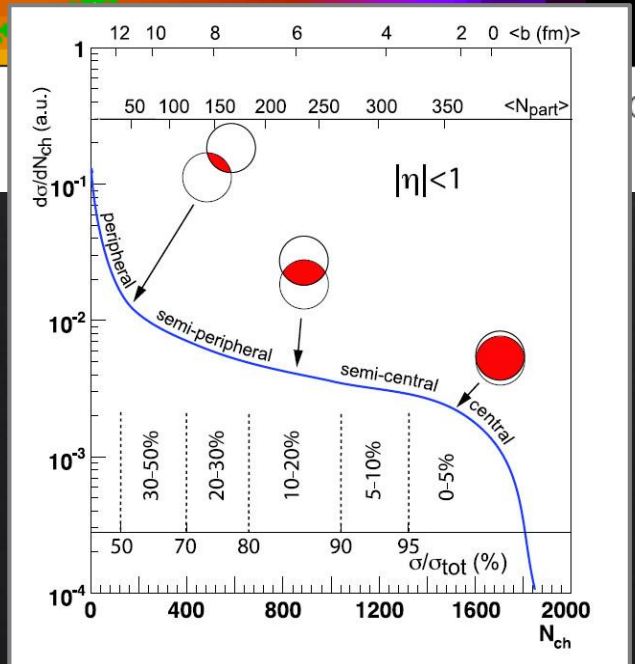


- correlation between N_{ch} at mid-rapidity and N_{part}
- large dispersion respect to AA collisions

p+Au collisions @ RHIC 200 GeV



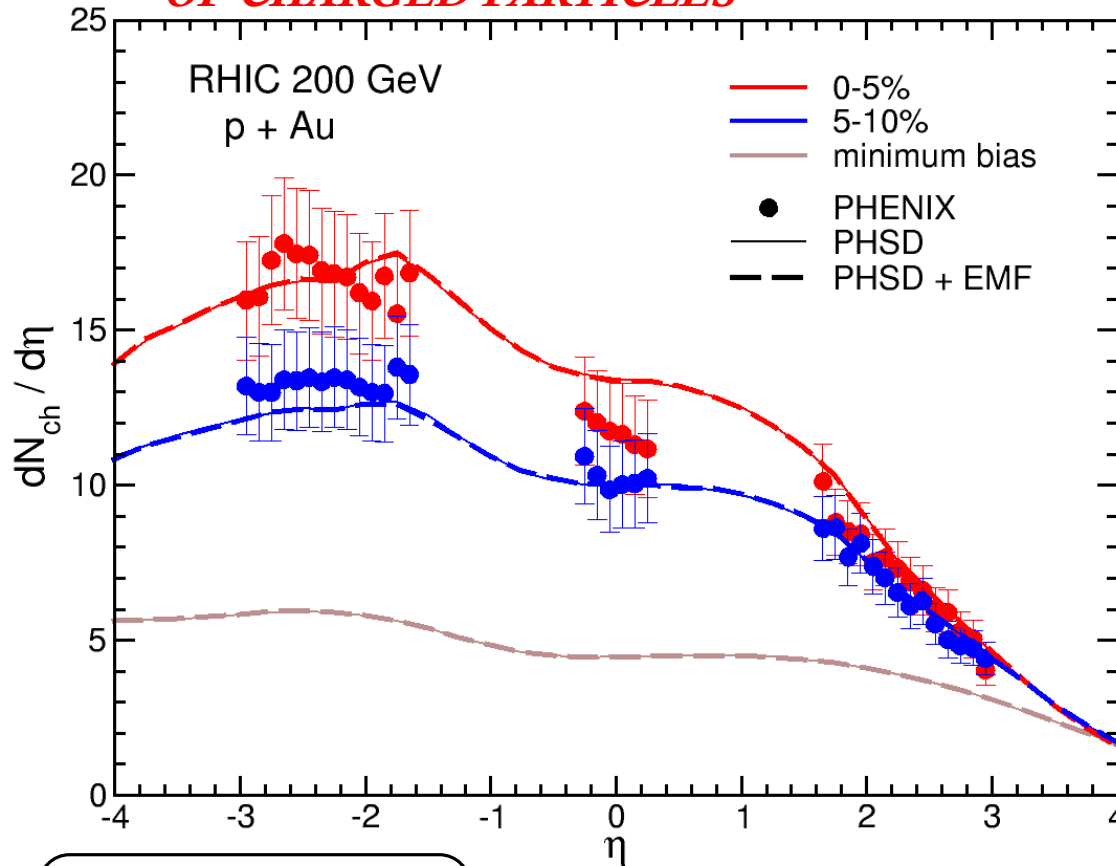
- correlation between N_{ch} at mid-rapidity and N_{part}
- large dispersion respect to AA collisions



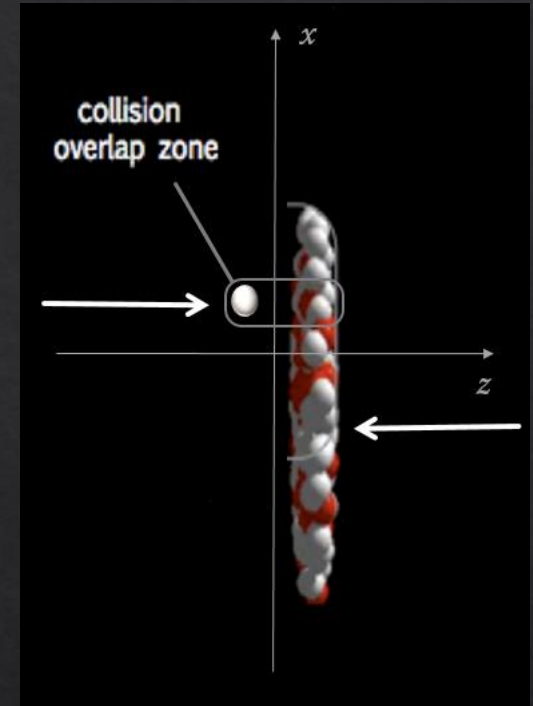
p+Au collisions @ RHIC 200 GeV

Exp. Data: PHENIX Collaboration, PRL 121 (2018) 222301

PSEUDORAPIDITY DISTRIBUTION OF CHARGED PARTICLES



$$\eta = -\ln\left(\tan\frac{\theta}{2}\right)$$

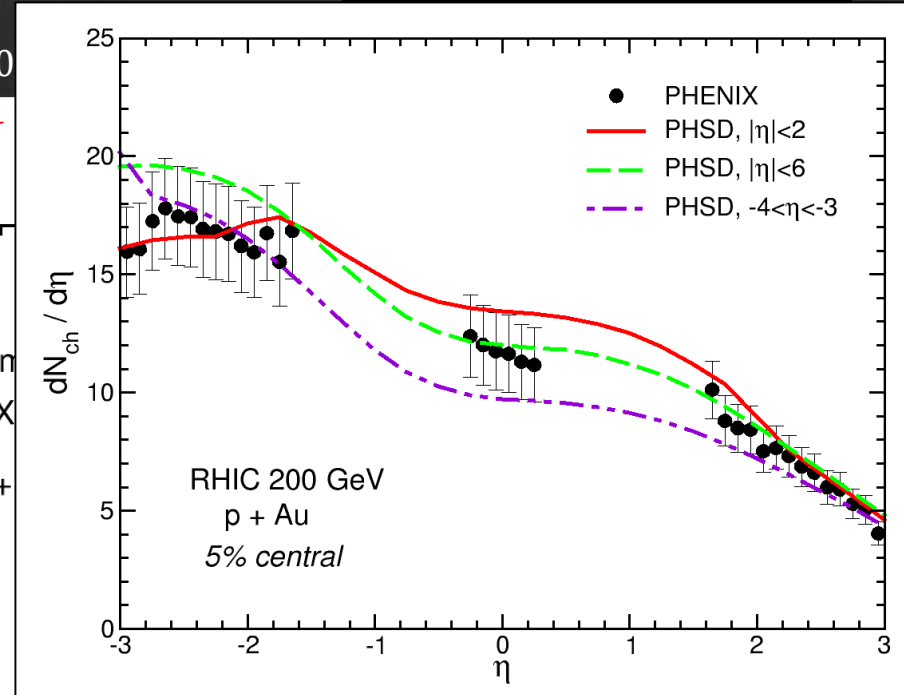
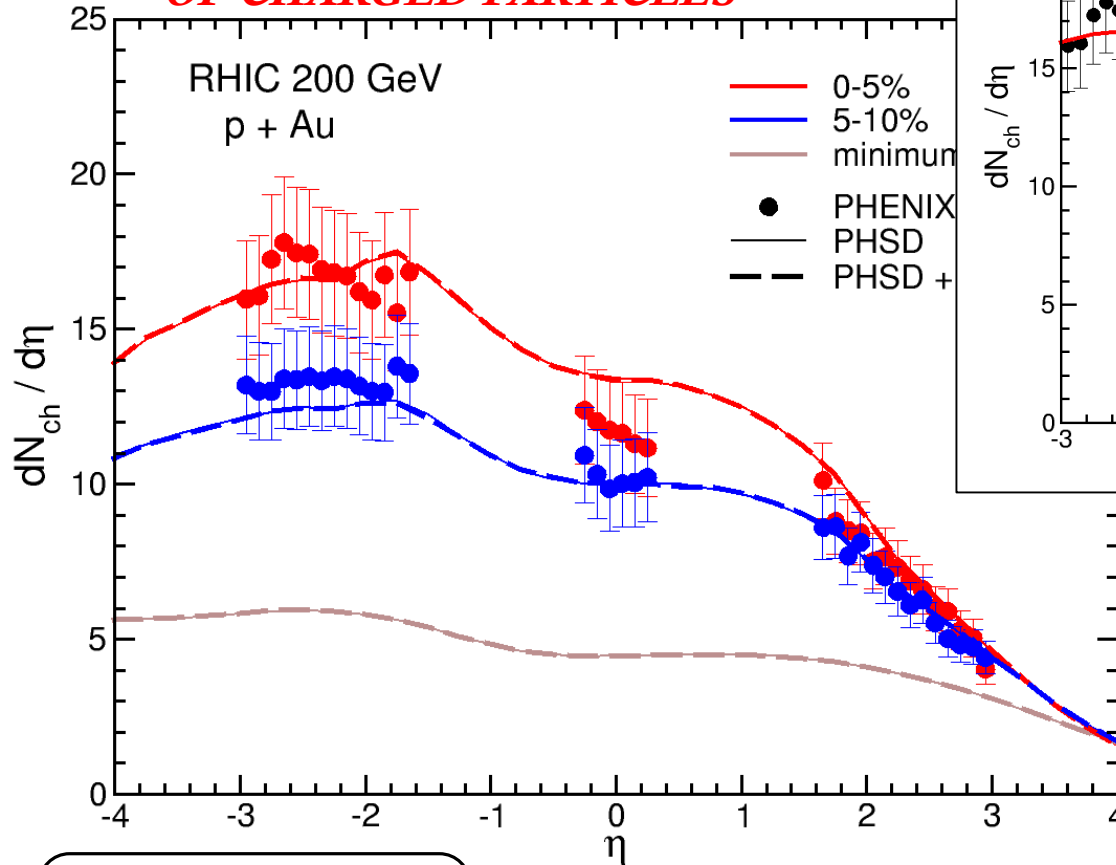


- enhanced particle production in the Au-going directions
- asymmetry increases with centrality of the collision

p+Au collisions @ RHIC 200 GeV

Exp. Data: PHENIX Collaboration, PRL 121 (2018) 22230

PSEUDORAPIDITY DISTRIBUTION OF CHARGED PARTICLES



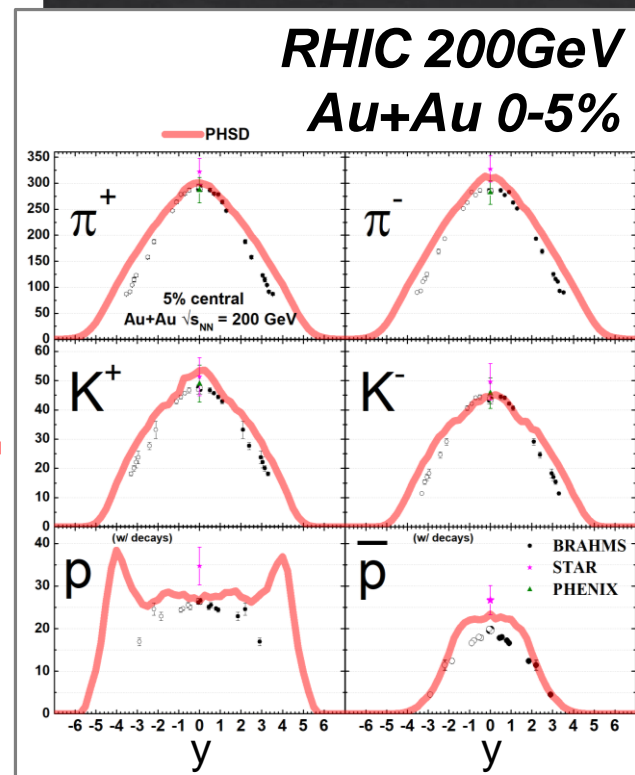
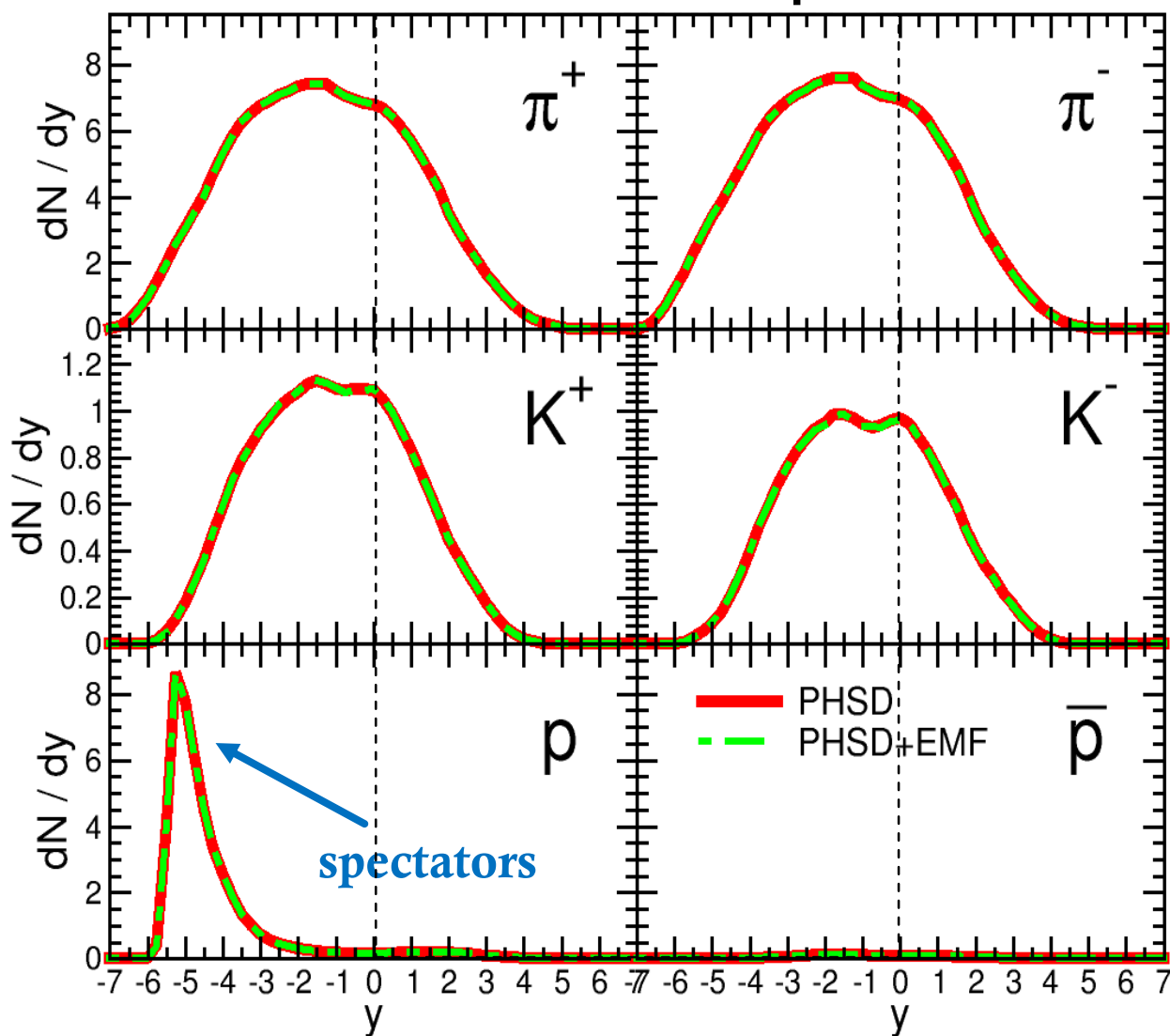
$$\eta = -\ln\left(\tan\frac{\theta}{2}\right)$$

- enhanced particle production in the Au-going directions
- asymmetry increases with centrality of the collision

p+Au collisions @ RHIC 200 GeV

RAPIDITY DISTRIBUTION OF IDENTIFIED PARTICLES

RHIC 200GeV
p+Au 0-5%

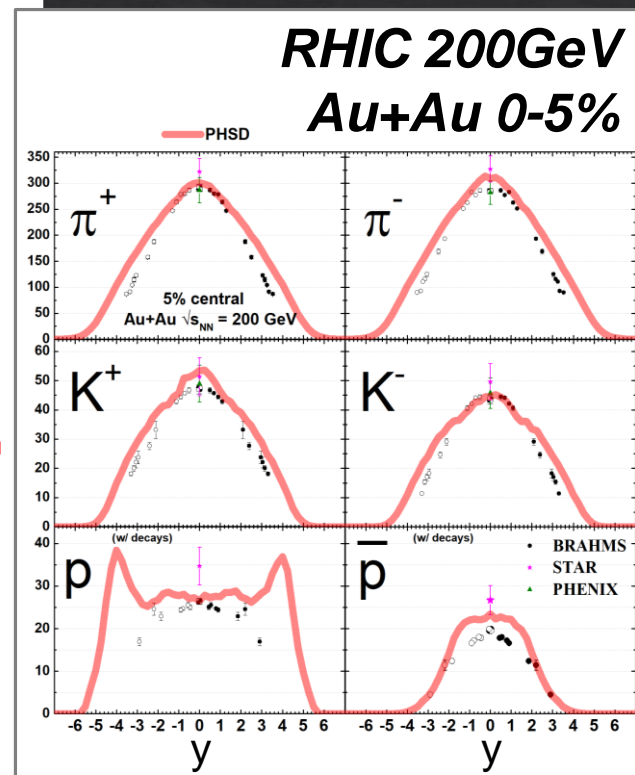
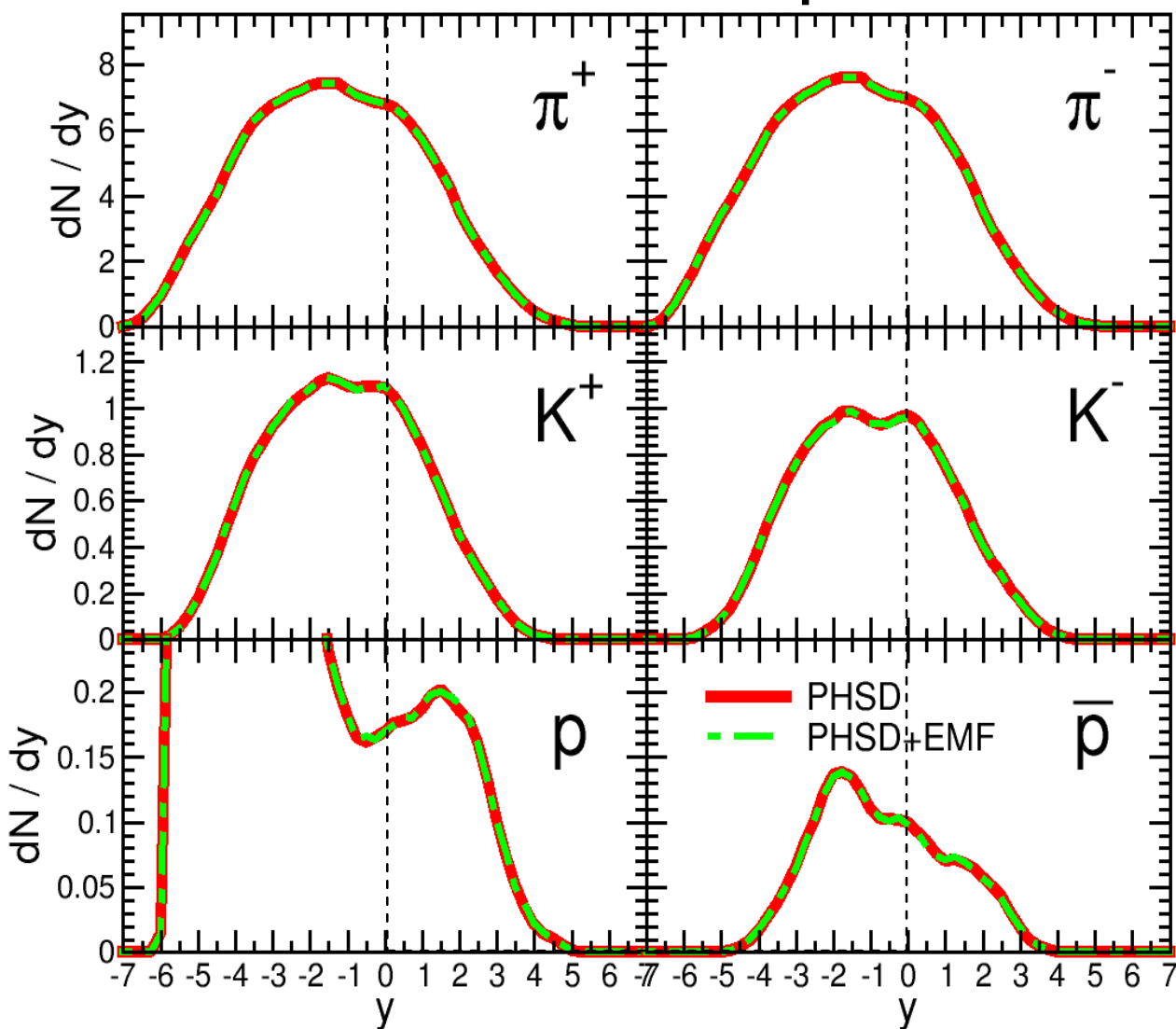


symmetric
colliding system

p+Au collisions @ RHIC 200 GeV

RAPIDITY DISTRIBUTION OF IDENTIFIED PARTICLES

RHIC 200GeV
p+Au 0-5%



symmetric
colliding system

Anisotropic radial flow

A DEEPER INSIGHT...INITIAL-STATE FLUCTUATIONS

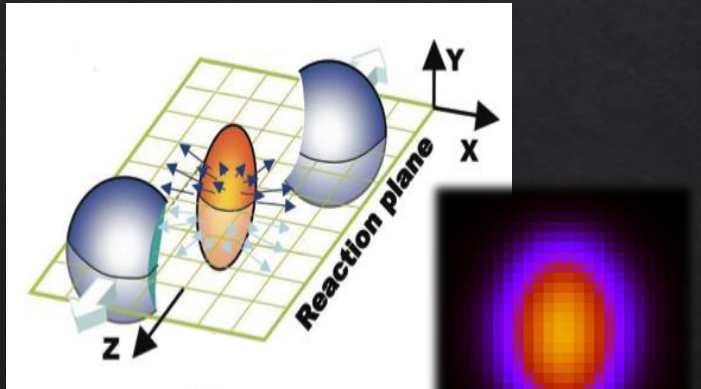


$$E \frac{d^3 N}{d^3 p} = \frac{1}{2\pi} \frac{d^2 N}{p_T dp_T dy} \left(1 + 2 \sum_{n=1}^{\infty} v_n(p_T, y) \cos(n(\phi - \Psi_r)) \right)$$

$$v_n = \langle \cos(n(\phi - \Psi_r)) \rangle$$

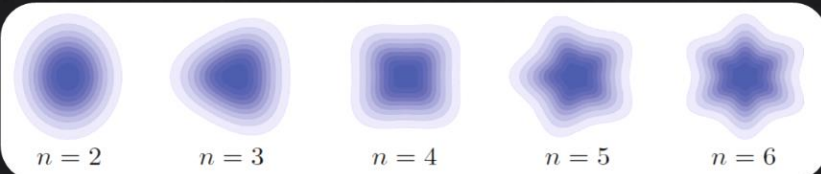
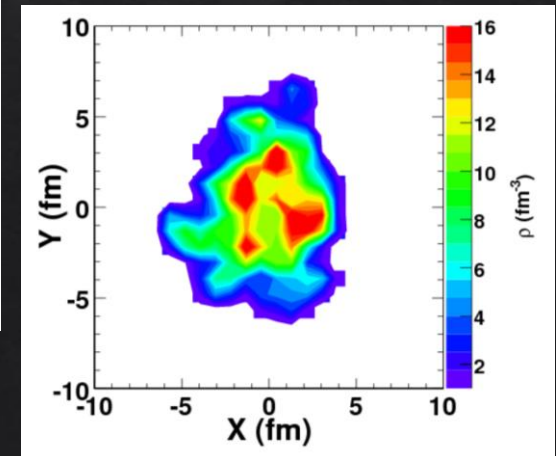
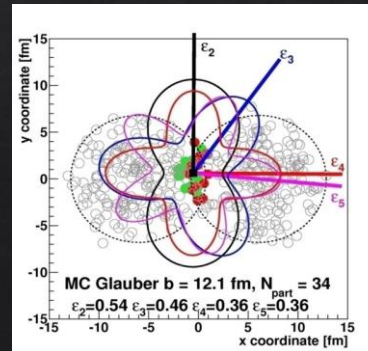
Not simply a smooth almond shape

➤ odd harmonics = 0



But a “lumpy” profile due to fluctuations of the position of nucleons in the overlap region

➤ odd harmonics $\neq 0$



Anisotropic radial flow

A DEEPER INSIGHT...FINITE EVENT MULTIPLICITY

azimuthal particle distributions
w.r.t. the reaction plane

$$\frac{dN}{d\varphi} \propto 1 + \sum_n 2v_n(p_T) \cos[n(\varphi - \Psi_n)]$$

Since the finite number of particles produces limited resolution in the determination of Ψ_n , the v_n must be corrected up to what they would be relative to the real reaction plane

Poskanzer and Voloshin,
PRC 58 (1998) 1671

n-th order
flow harmonics

$$v_n = \frac{\langle \cos[n(\varphi - \Psi_n)] \rangle}{\text{Res}(\Psi_n)}$$

n-th order
event-plane angle

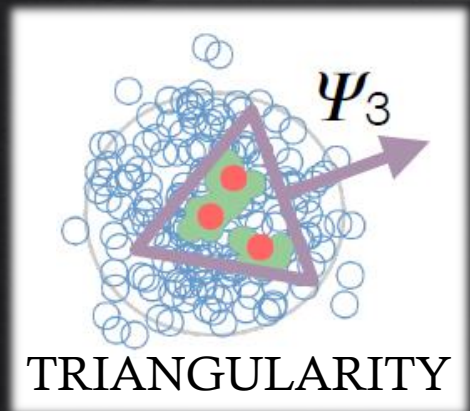
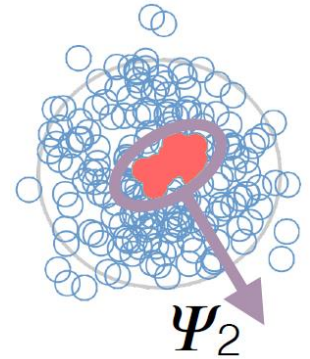
$$\Psi_n = \frac{1}{n} \text{atan2}(Q_n^y, Q_n^x)$$

$$Q_n^x = \sum_i \cos[n\varphi_i]$$

$$Q_n^y = \sum_i \sin[n\varphi_i]$$

event-plane angle resolution
(three-subevent method)

ELLIPTICITY



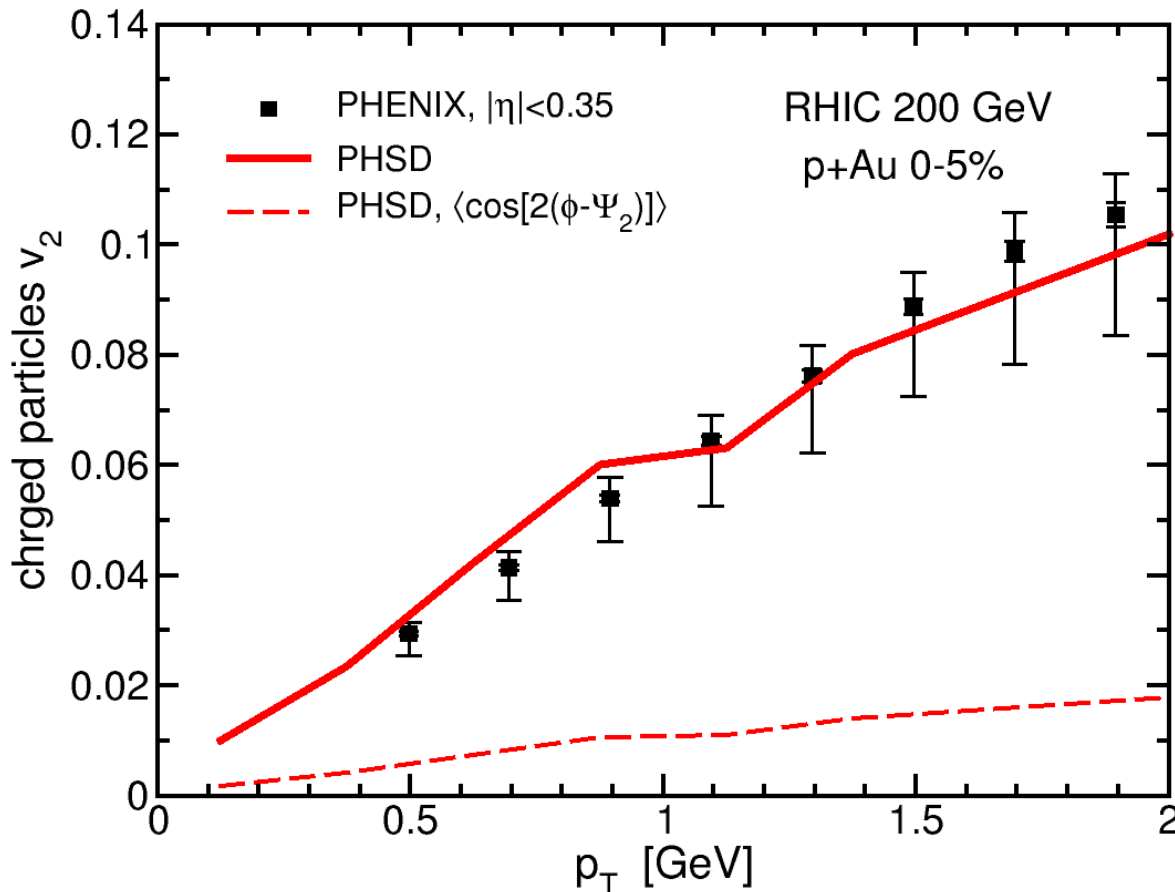
TRIANGULARITY

Important especially for small
colliding system, e.g. p+A

p+Au collisions @ RHIC 200 GeV

ELLIPTIC FLOW OF CHARGED PARTICLES

$$v_2(p_T) = \frac{\langle \cos[2(\phi(p_T) - \Psi_2)] \rangle}{Res(\Psi_2)}$$

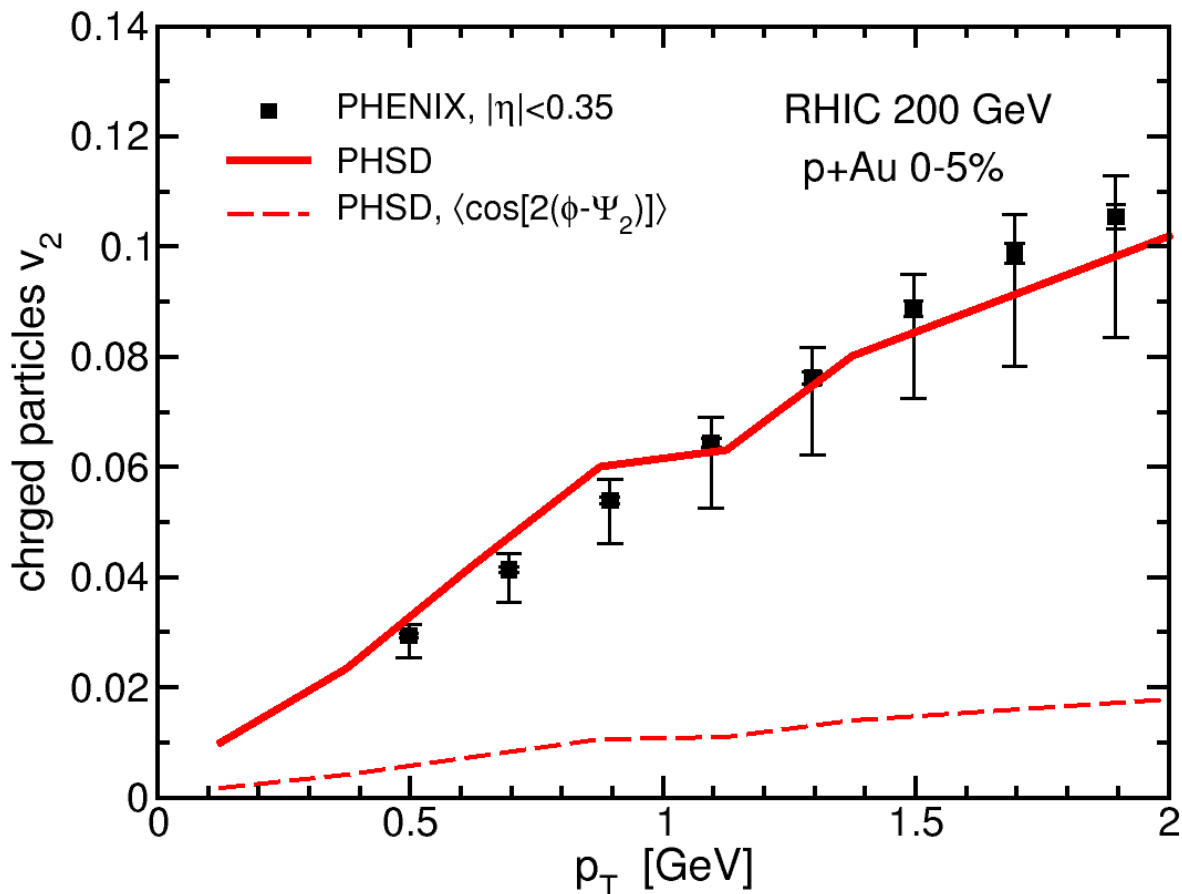


Event-plane angle
in $-3 < \eta < -1$:
 $Res(\Psi_2^{PHSD}) = 0.175$
 $Res(\Psi_2^{PHENIX}) = 0.171$

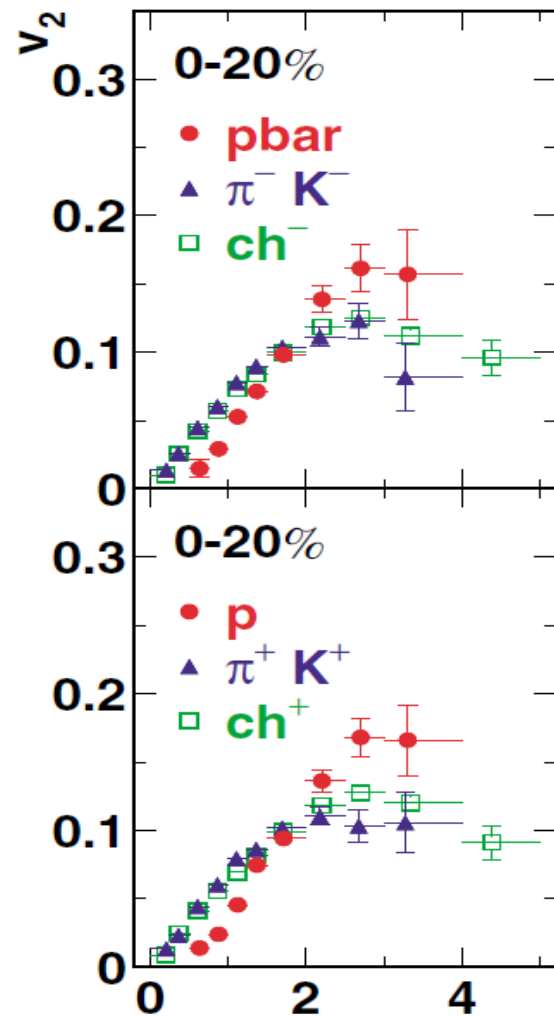
- Magnitude correlated with the determination of the reaction plane
- Comparable to that found in collisions between heavy nuclei
- Indicate the formation of short-lived droplets of quark-gluon plasma

p+Au collisions @ RHIC 200 GeV

ELLIPTIC FLOW OF CHARGED PARTICLES



RHIC 200GeV Au+Au



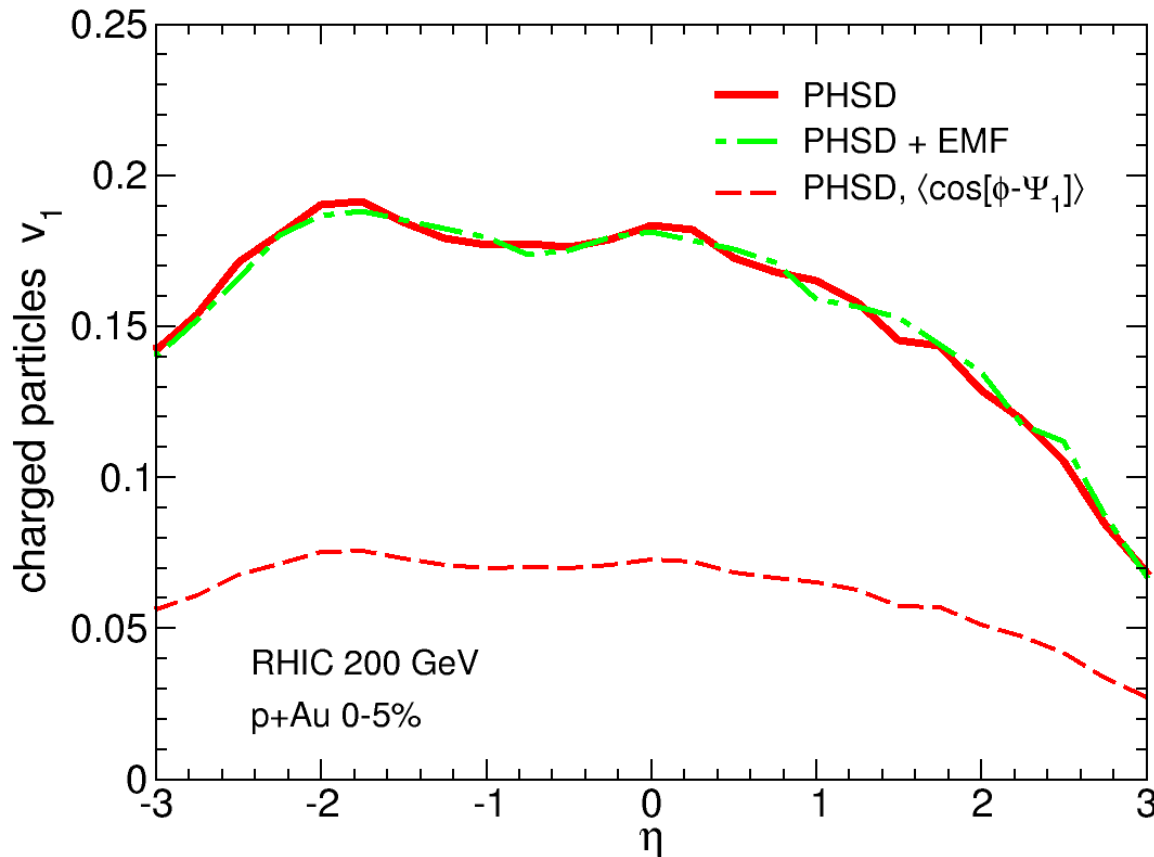
p+Au collisions @ RHIC 200 GeV

PRELIMINARY

*pseudorapidity dependence of the
DIRECTED FLOW OF
CHARGED PARTICLES*

$$v_1(\eta) = \frac{\langle \cos[\varphi(\eta) - \Psi_1] \rangle}{Res(\Psi_1)}$$

Event-plane angle
in $-4 < \eta < -3$:
 $Res(\Psi_1^{PHSD}) = 0.397$

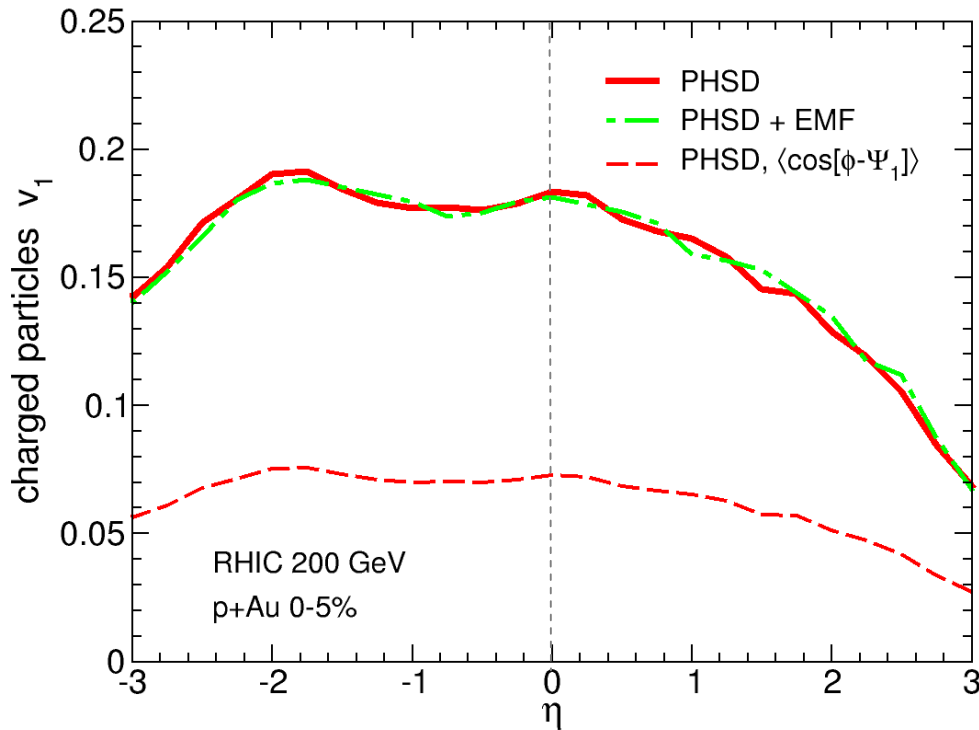


- Magnitude correlated with the determination of the reaction plane
- Stronger with respect to heavy ion collisions
- mainly due to initial-state fluctuations
- probably no effect of vorticity

p+Au collisions @ RHIC 200 GeV

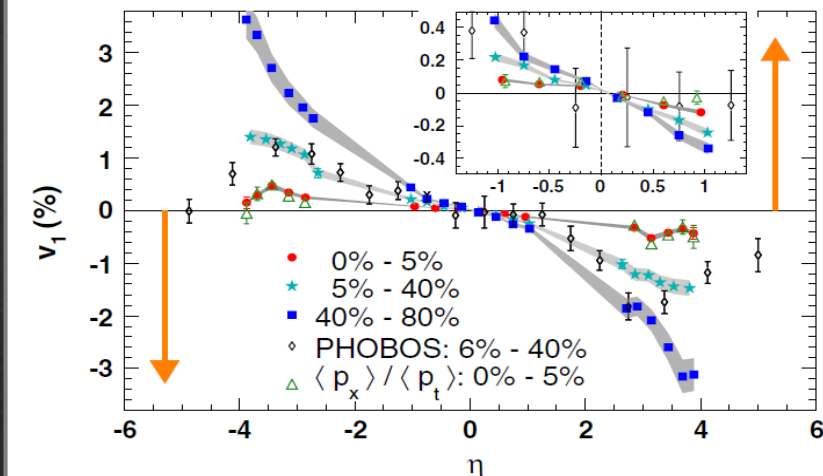
PRELIMINARY

**pseudorapidity dependence of the
DIRECTED FLOW OF
CHARGED PARTICLES**

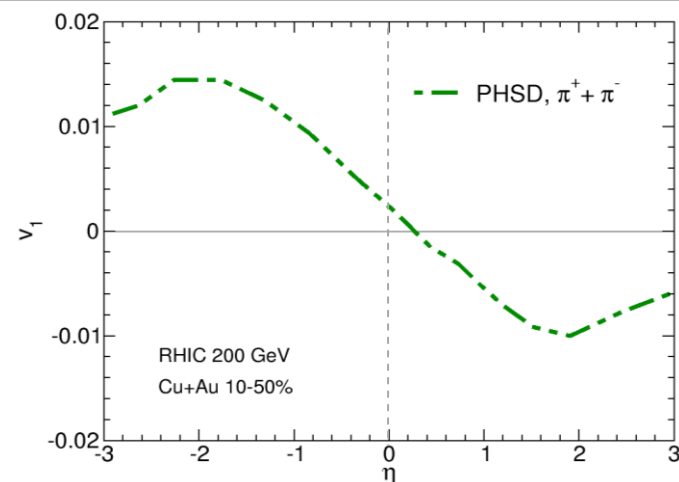


RHIC 200GeV p+Au

STAR Collaboration, PRL 101 (2008) 252301



RHIC 200GeV Au+Au



RHIC 200GeV Cu+Au

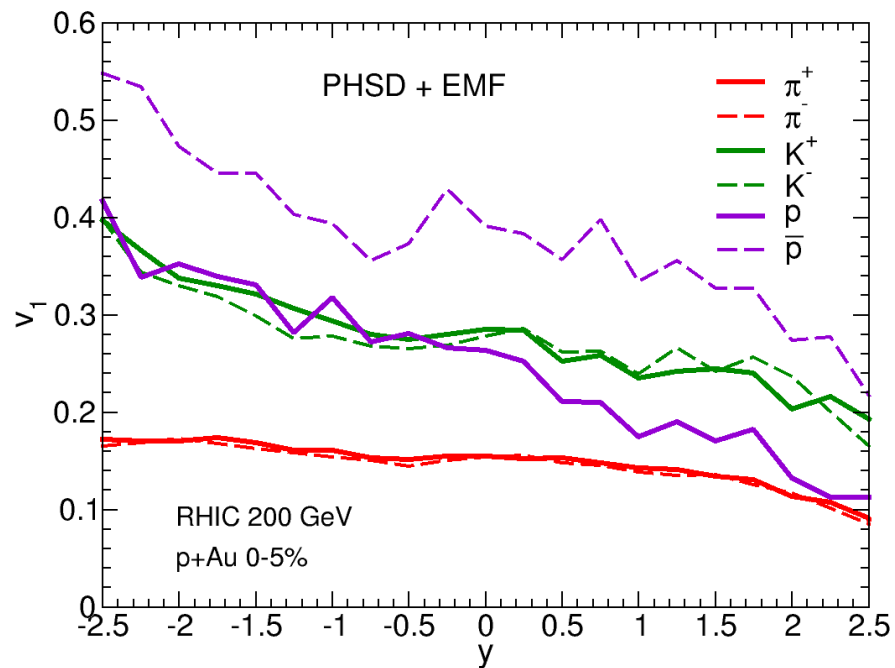
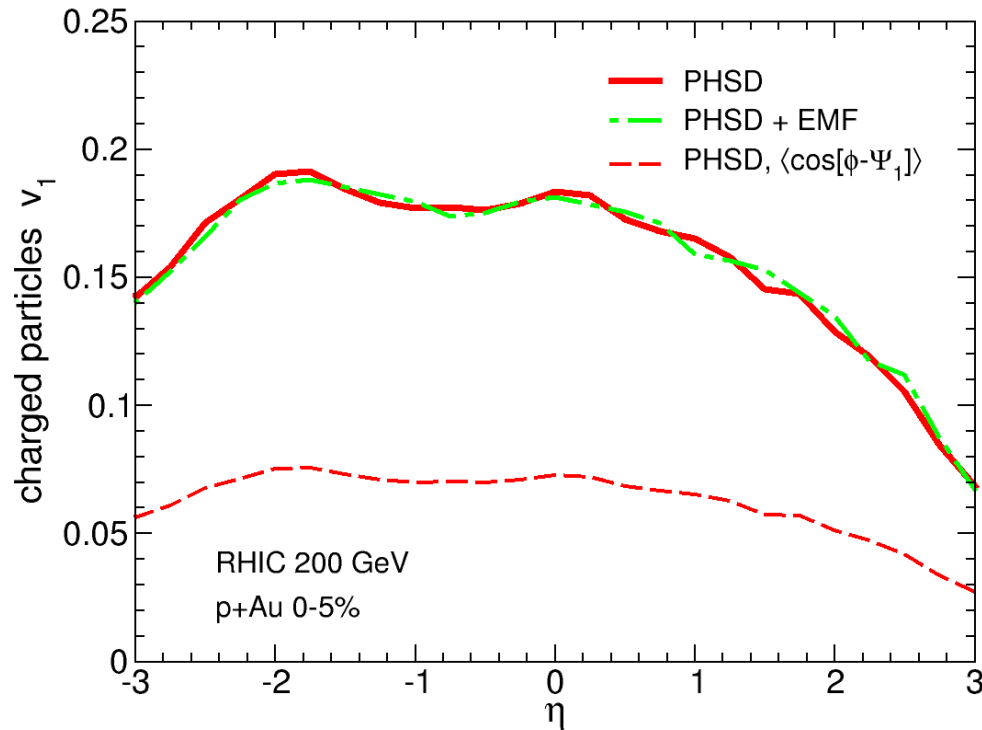
Voronyuk *et al.*, PRC 90 (2014) 064903

Toneev *et al.*, PRC 95 (2017) 034911

p+Au collisions @ RHIC 200 GeV

PRELIMINARY

*pseudorapidity dependence of the
DIRECTED FLOW OF
IDENTIFIED PARTICLES*



- Splitting of positively and negatively charged particles induced by the electromagnetic field?
- NO visible splitting in $v_1(y)$
- Looking at $v_1(p_T)$ and charm mesons...

CONCLUDING....

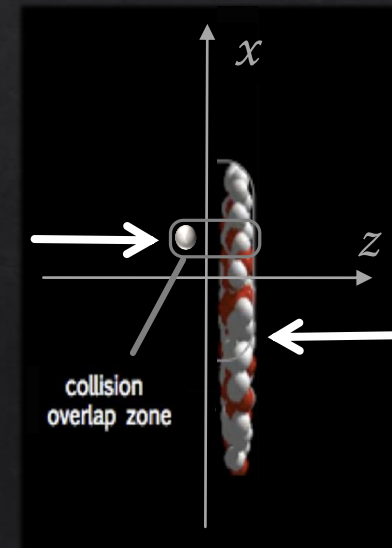


The Parton-Hadron-String-Dynamics (PHSD) describes the entire dynamical evolution of heavy ion collisions within one single theoretical framework

PHSD includes in a consistent way the intense electromagnetic fields produced in the very early stage of the collision

Study of p+Au collisions at top RHIC energy:

- ✓ the electric field is strongly asymmetric inside the overlap region
- ✓ asymmetry of charged-particle rapidity distributions increasing with centrality
- ✓ collectivity as signal of quark-gluon plasma formation
- ✓ stronger directed flow respect to symmetric colliding system
- ✓ no clear effect of electromagnetic fields on hadronic observables



**Thank you
for your attention!**

DQPM: Dynamical QuasiParticle Model

The QGP phase is described in terms of interacting quasiparticle: massive quarks and gluons (g, q, \bar{q}) with Lorentzian spectral functions

$$\rho_j(\omega, \mathbf{p}) = \frac{\gamma_j}{\tilde{E}_j} \left(\frac{1}{(\omega - \tilde{E}_j)^2 + \gamma_j^2} - \frac{1}{(\omega + \tilde{E}_j)^2 + \gamma_j^2} \right) \equiv \frac{4\omega\gamma_j}{(\omega^2 - \mathbf{p}^2 - M_j^2)^2 + 4\gamma_j^2\omega^2}$$

■ **quarks**

mass: $m^2(T) = \frac{N_c^2 - 1}{8N_c} g^2 \left(T^2 + \frac{\mu_q^2}{\pi^2} \right)$

width: $\gamma_q(T) = \frac{N_c^2 - 1}{2N_c} \frac{g^2 T}{4\pi} \ln \frac{c}{g^2}$

running coupling: $\alpha_s(T) = g^2(T)/(4\pi)$

$$g^2(T/T_c) = \frac{48\pi^2}{(11N_c - 2N_f) \ln(\lambda^2(T/T_c - T_s/T_c)^2)}$$

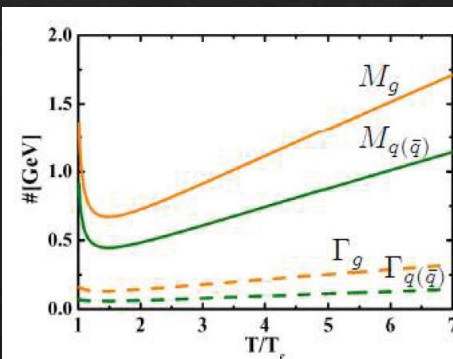
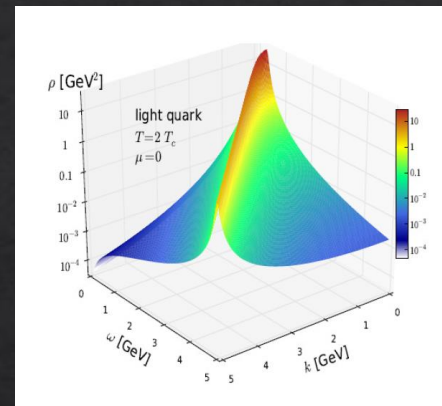
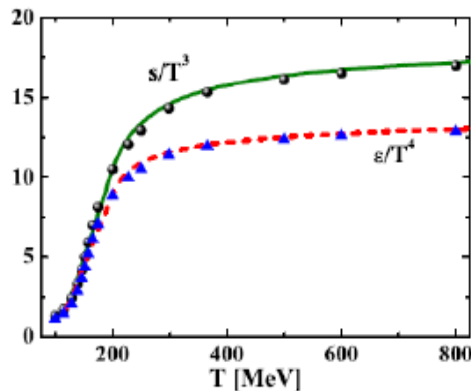
➤ **fit to lattice (IQCD) results** (e.g. entropy density)

with 3 parameters: $T_s/T_c=0.46$; $c=28.8$; $\lambda=2.42$

■ **gluons:**

$M^2(T) = \frac{g^2}{6} \left((N_c + \frac{1}{2}N_f) T^2 + \frac{N_c}{2} \sum_q \frac{\mu_q^2}{\pi^2} \right)$ $N_c = 3, N_f = 3$

$\gamma_g(T) = N_c \frac{g^2 T}{4\pi} \ln \frac{c}{g^2}$



Peshier, PRD 70 (2004) 034016

Peshier and Cassing, PRL 94 (2005) 172301

Cassing, NPA 791 (2007) 365; NPA 793 (2007)